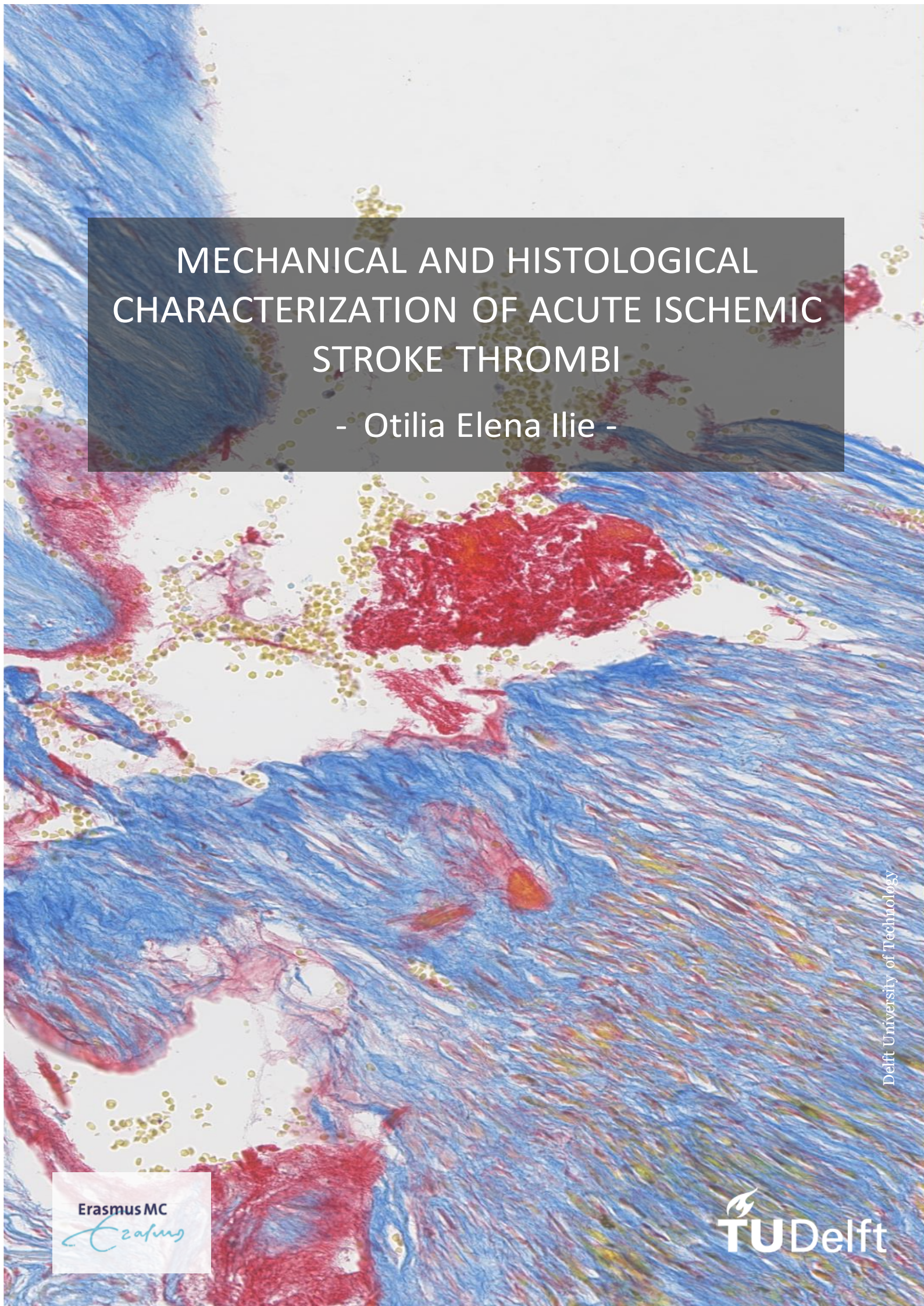

MECHANICAL AND HISTOLOGICAL CHARACTERIZATION OF ACUTE ISCHEMIC STROKE THROMBI

- Otilia Elena Ilie -

Delft University of Technology

Erasmus MC

TU Delft

Mechanical and histological characterization of acute ischemic stroke thrombi in relation to EVT procedure

by

Otilia Elena Ilie

to obtain the degree of

Master of science in Biomedical Engineering

at the Delft University of Technology,

to be presented on the 19th of July.

Student number:	5629268
Supervisors:	Dr.ir. Frank Gijsen
	Dr. Behrooz Fereidoonnezhad
Thesis Committee:	Dr.ir. Frank Gijsen
	Dr. Behrooz Fereidoonnezhad
	PhD. Luca Bontempi

TU Delft

Contents

Acknowledgements
1. Scientific paper 1
1. Introduction 2
2. Methods 2
2.1. Patient inclusion 2
2.2. Endovascular thrombectomy procedure 3
2.3. Thrombus collection and preparation of thrombus samples 3
2.4. Mechanical characterization 4
2.5. Histological analysis 5
2.6. Statistical analysis 6
3. Results 6
3.1. Patients clinical and interventional data 6
3.2. Thrombus composition 6
3.3. Mechanical properties 8
3.4. Composition in relation to mechanical properties 10
4. Discussion 12
5. Limitations 14
6. Conclusion 15
7. References 15
2. Annexes 17
A. Thrombus samples 17
A1. Collection 17
A2. Preparation 18
A3. Protocol samples preparation 18
A4. Additional results 20
B. Mechanical testing 21
B1. Signal processing 22
B2. Reasons for exclusion of data 23
B3. Protocol unconfined compression test 25
B4. Results 25
C. Histology 27
C1. Methods 27
C2. Protocol histology samples 29
C3. Results 31
D. Mechanical properties and composition 34
F. MATLAB scripts 37

Acknowledgements

I would like to express my thanks to my thesis supervisor, Behrooz Fereidoonnezhad, for giving me the opportunity to take on this project. My deepest gratitude goes to my daily supervisor, Frank Gijsen, for his unwavering support, guidance, and invaluable feedback guiding me through the research process and my academic journey.

I extend my sincere thanks to the BME department staff at Erasmus MC, particularly to Kim van Gaalen and Robert Beurskens, whose expertise and technical assistance were invaluable for this research. Their mentorship extended beyond the laboratory, offering invaluable personal advice and support during challenging times. I also want to acknowledge the dedication of my other BME department colleagues, whose commitment to education and research enriched my academic experience.

Special recognition is due to the interventionalists in the Radiology department, whose collaboration was essential for the success of this research. I am deeply grateful to all participants in this study, especially Stephanie Nadin ten Cate, whose dedication and hard work were indispensable. Together, we navigated long hours in the lab, facing challenges with resilience and supporting each other through stressful times.

To my dear friends Tracy Chenrui Zhang and Malisa Sun, I owe a debt of gratitude for their unwavering support and encouragement throughout my master's journey. Your friendship has been a source of strength and solace during the most intense periods of research, and I am profoundly grateful for your presence in my life.

Lastly, I am profoundly grateful to my family for their unconditional love, unwavering encouragement, and unwavering support throughout my journey. Their steadfast presence and understanding helped me navigate the challenges of relocating to another country and remained focused on my academic pursuits while still finding time to take care of myself. Their belief in me never wavered, and for that, I am forever thankful.

1

Scientific paper

Mechanical and histological characterization of acute ischemic stroke thrombi in relation to EVT procedure

Authers: Otilia Elena Ilie[1], Frank Gijsen[2],
[1]Delft University of Technology, [2]Erasmus Medical Center Rotterdam

Background: Ischemic stroke remains a major global health threat and a leading cause of mortality. Although advancements have been made in acute ischemic stroke treatment, challenges persist in achieving efficient recanalization and improved outcomes. Research on the mechanical characterization of ex vivo thrombi is limited. This paper aims to investigate the compositional and mechanical characterization of acute ischemic stroke thrombi retrieved in a per pass method and determine the relationship between composition and mechanical properties.

Methods: Thrombi fragments were collected per pass and segmented into samples. Larger fragments were sectioned into 1 mm pieces for cyclic unconfined compression testing, assessing hysteresis and tangent modulus as a measure of stiffness. The remaining pieces post-sectioning were combined into a single offcut sample, while smaller fragments were labeled as extra samples and kept for histology. Following mechanical testing, compositional analyses quantified the percentages of red blood cells, fibrin, and platelets in each sample.

Results: In 34 passes, a total of 108 thrombus fragments from 20 patients were successfully retrieved. Compositional heterogeneity was observed both between patients and within a single patient. Higher red blood cells (RBC) and lower fibrin/platelet contents were associated with Pass 1. The results showed a mean hysteresis area of 1.6 kPa and a mean hysteresis ratio of 37%. The median low strain stiffness was 1.76 kPa and the median high strain stiffness was 576.4 kPa. RBC and fibrin/platelets concentration had a linear relationship with high strain stiffness. Low strain stiffness, hysteresis area, and ratio changed with varying quantities of fibrin/platelets, RBC, and platelets composition.

Conclusion: This study enhances understanding of the relationship between thrombus composition and mechanical properties. The findings highlight the significant heterogeneity in thrombi and the non-linear viscoelastic behavior. Stiffness is highly corelated to strain levels, and the hysteresis amount depends on structural changes and varying compositional concentrations.

1. Introduction

Stroke ranks as one of the leading causes of mortality globally, with ischemic strokes accounting for 62% of all stroke incidents, amounting to over 7.6 million new cases annually [1]. Despite significant advancements, achieving complete recanalization—a crucial factor for recovery, defined by a modified Treatment in Cerebral Infarction score of 3—remains unattainable in 30% of acute ischemic stroke (AIS) cases, often resulting in poor outcomes [2]. Factors impeding recanalization include the challenging access to and retrieval of thrombi, exacerbated by their varying composition and mechanical properties.

Research into the physical properties of AIS thrombi, specifically their compression stiffness and tensile strength, is scant yet crucial, as these properties significantly influence the efficacy of mechanical thrombectomy (MT) [3] [4] [5]. Studies indicate that thrombi heterogeneity contributes to a range of mechanical behaviors during MT, with thrombi rich in fibrin and platelets showing greater stiffness, leading to longer procedure times and lower recanalization scores. This is quantified as a 9 kPa increase in thrombus stiffness (elastic modulus at 75% strain) for each 1% increase in fibrin/platelets [3]. Conversely, thrombi with a high red blood cell content are typically softer and easier to retrieve [3]. Moreover, a high granulocyte count within thrombi is associated with increased stiffness and MT failure, suggesting a direct impact on recanalization success [5]. These complexities highlight the need for more research to improve our understanding of thrombus behavior during MT and enhance treatment outcomes.

The primary aim of this research is to characterize the composition and mechanical properties of AIS thrombi, focusing on bridging the gap between these two aspects, adopting a per-pass approach.

2. Methods

2.1. Patient inclusion

Thrombi were collected from patients who underwent endovascular thrombectomy (EVT) for acute ischemic stroke at Erasmus Medical Centre in Rotterdam between August 2022 to July 2023. The inclusion criteria encompassed patients with the following specifics: 18 years or over, diagnosed with proximal intracranial occlusion of the anterior

circulation (ICA, ICA-terminus, M1, M2 and M3) as confirmed on admission computed tomography angiography, and had successful retrieval of thrombus material in at least one procedural pass.

This study was conducted within the framework of the MRCLOT clinical trial, which received approval from the medical ethics committee of the Erasmus Medical Center Rotterdam. All patients provided written informed consent for the collection of tissue material, mechanical testing, and histological analysis of retrieved thrombi.

2.2. Endovascular Thrombectomy procedure

MT was primarily performed under conscious sedation, and frontline thrombectomy strategies, such as Stent Retriever (SR), Contact Aspiration (CA), Balloon catheter, or a combination thereof, were chosen by the neuro-interventionalist. Thrombus material collection during MT followed a per-pass approach, with thrombus fragments collected separately for each procedural pass. To maintain cellular integrity, the retrieved fragments were stored in containers filled with Dulbecco's Modified Eagles Medium (DMEM) and kept at 4-10°C. Subsequently, the neuro-interventionalist completed an intervention form, documenting procedural details, including frontline strategy, number of device passes, successful recanalization rate (measured by modified Thrombolysis in Cerebral Infarction (mTICI) 2b-3), and puncture to reperfusion duration.

2.3. Thrombus collection and preparation of thrombus samples

The tissue material was promptly collected from the Angio suite after completion of the MT operation. Thrombi fragments from each pass were photographed alongside a ruler and labeled for identification. Fragments deemed too small for effective testing were put aside for histology and labeled as 'extra' samples. Apon visual inspection, depending on the thickness of the thrombus fragments, the large pieces were cut into 1 mm or 2 mm thick slices, with two flat parallel faces to facilitate mechanical testing (see Figure 1). The distal and proximal end parts of the fragments, together with the rest of unused slices were combined into a single histology sample labeled as 'offcuts'. Figure 1 illustrates the preparatory steps for obtaining mechanical samples from the retrieved thrombi fragments.

Multiple samples per patient were cut for mechanical testing. Each of those samples were photographed next to a ruler for cross-sectional area (CSA) measurements using Image J software. After cutting and mechanical testing, all samples (extra, offcuts, mechanical samples) were preserved in HEPES (Sigma-Aldrich) buffer solution and processed for compositional analysis as soon as possible.

Thrombus material was mechanically tested and fixated for histology within a maximum period of 6 hours following the MT procedure. Additional details regarding the preparation of samples can be found in Annex A.

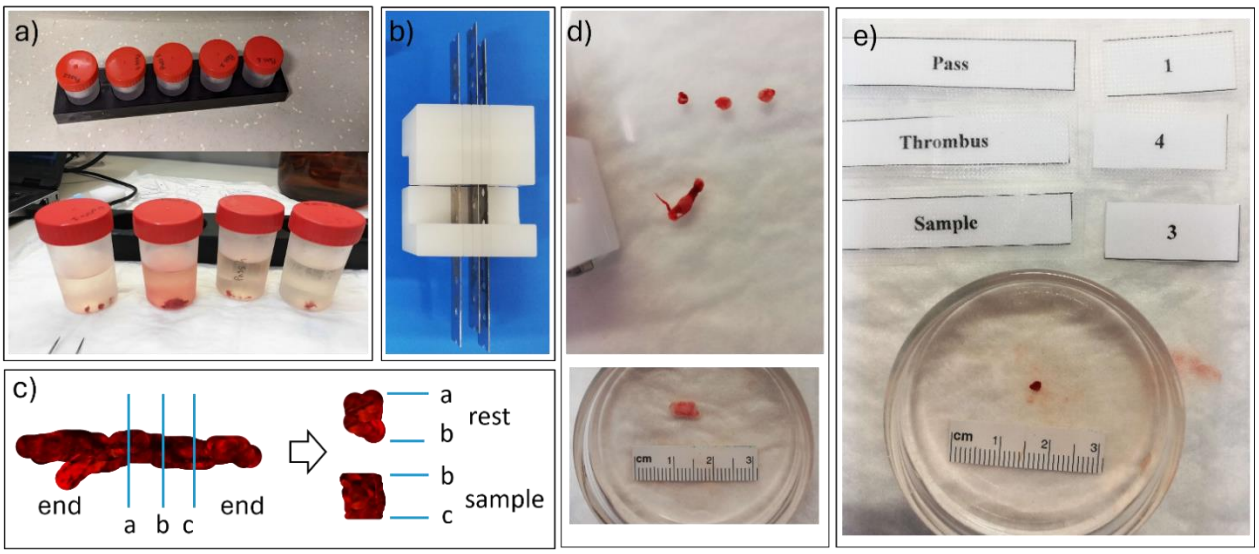

Figure 1: Samples preparation: a) Containers with thrombus fragments per pass; b) Mold and blades used for slicing; c) Diagram showing a thrombus fragment sectioned for mechanical samples, with end and rest parts pieces labeled as one 'offcut sample'; d) Examples of thrombus fragments; e) One mechanical sample.

2.4. Mechanical characterization

To mechanically characterize acute ischemic stroke thrombi, three main properties were determined: stiffness at low and high strain, and hysteresis. Assessing stiffness at low strain provides a baseline measure prior to any structural changes that can occur at higher strains. Additionally, it can be representative of the small deformations within the vascular system and indicate how easy a thrombus can deform, potentially migrating within the bloodstream. Higher strain stiffness was chosen because it can indicate the mechanical integrity and force resistance of the thrombus, which are essential in designing new retrieval devices with specific pull-out forces that can easily achieve recanalization [6]. Lastly, the hysteresis area and ratio were also measured to determine the energy dissipation under cyclic loading, specific for viscoelastic biological tissue.

Unconfined compression test was used to extract all these properties. This technique has been proven suitable for assessment of both human clot analogues and AIS retrieved thrombi, providing accurate and reproducible data on their mechanical properties [6] [3].

A custom-built compression device, as previously described [3], was used to run the mechanical testing. Figure 2a illustrates the equipment. A load cell of 2.5 N (LSB200 Jr. Miniature S-beam, Futek) was used to compress the samples to 80% of their original height over 20 cycles at a rate of 0.1 mm/s. Prior to testing, samples were equilibrated for 5 minutes in a water bath with HEPES buffer solution at 37°C and remained submerged during the test to simulate physiological conditions. It was considered that the samples were already subjected to multiple forces during the EVT procedure due to the interaction with either a SR or aspiration catheter, thus no further pre-conditioning force was applied before testing the samples under compression.

The response force and tissue deformation were recorded on a force-time curve and subsequently converted to nominal stress-strain values using the cross-sectional area of the samples (Figure 2b and c). Tangent modulus at low and high strains was determined by linear fitting to the initial 10% and final 5 % of the stress-strain curve. These points were selected based on typical stress-strain curve characteristics shown in Figure 2c. The curve initiates with an early linear portion (up to approximately 30% strain), transitions into a non-linear region indicating material stiffening, and concludes with a final linear phase [7].

Loading and unloading stress-strain curves of each cycle were used to plot the hysteresis (Figure 2c) and measure the hysteresis area (the area between the two curves) and hysteresis ratio (defined as the ratio between the hysteresis area and the total area under loading curve).

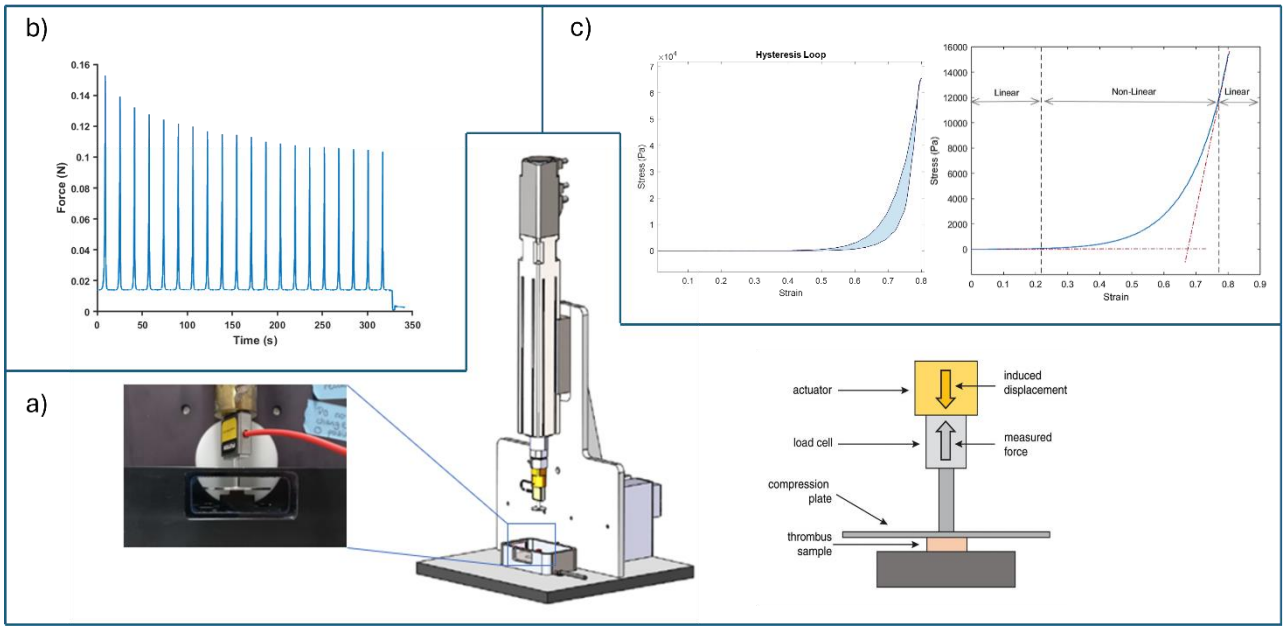

Figure 2: a) Design of the compression tester, featuring a close-up view of a sample under the compression plate in a water bath (Updated from Boodt et al. [3]); b) Force-time signal curve along the 20 cycles; c) Hysteresis of one cycle and detail of the first loading curve showing the initial linear phase, followed by a non-linear stiffening curve, and concluding with a higher linear phase.

During the experiments, several samples were subjected to 60% compression instead of 80%. To be able to use the data from these samples and ensure integrity of the final analysis, a Gaussian extrapolation was employed to extend the stress-strain curve to 80%, allowing measurements of high strain stiffness. For additional details of mechanical experimental protocol and signal processing, check Annex B.

2.5. Histological analysis

After mechanical testing, all samples, including offcuts and non-viable fragments, were immersed in formaldehyde (3.8-4.2% HCOH) for at least 24 hours to achieve fixation. Subsequently, the samples underwent dehydration and embedding in separate paraffin blocks. A minimum of 6 consecutive sections of 5 µm thickness were cut (2 sections per slide). Representative slides from each block were subjected to Hematoxylin and Eosin (H&E), Martius Scarlet Blue (MSB), and Immunohistochemical CD42b staining, as shown in figure 3. The stained slides were scanned using a high-definition Nanozoomer (NDP.view2, Hamamatsu Nano-Zoomer, Hamamatsu Photonics K.K., Japan) at a resolution of 40x0.23 µm/pixel.

Histological quantification was carried out on the digital slide images using Orbit Image Analysis Software (Orbit, Idorsia Ltd.; www.Orbit.bio), as previously described [8]. MSB and CD42b staining were primarily used to determine the proportion of red blood cells (RBC), fibrin with platelets, and platelets, expressed as a percentage of the respective color area. Given the high number of samples and the fact that white blood cells (WBCs) typically constitute only 2-4% of thrombus composition, WBC quantification was not conducted in this study [9]. An experienced pathologist, blinded to the interventional and clinical information of patients, verified the composition quantification made in Orbit.

The MSB quantification results were used for the final data analysis and correlation with mechanical and procedural variables. This decision was based on the limitations of H&E staining, such as low specificity and poor color distinction between components, making automatic quantification difficult (see Annex C, Figure C2). One the other hand, MSB is considered more suited for stroke thrombus composition, due to the distinct coloration of components, that allows easier and more precise quantification (Figure 3) [10]. Therefore, the H&E measurements were used as a validation step for the MSB results. For a comprehensive overview of histology and image analysis, please refer to Annex C.

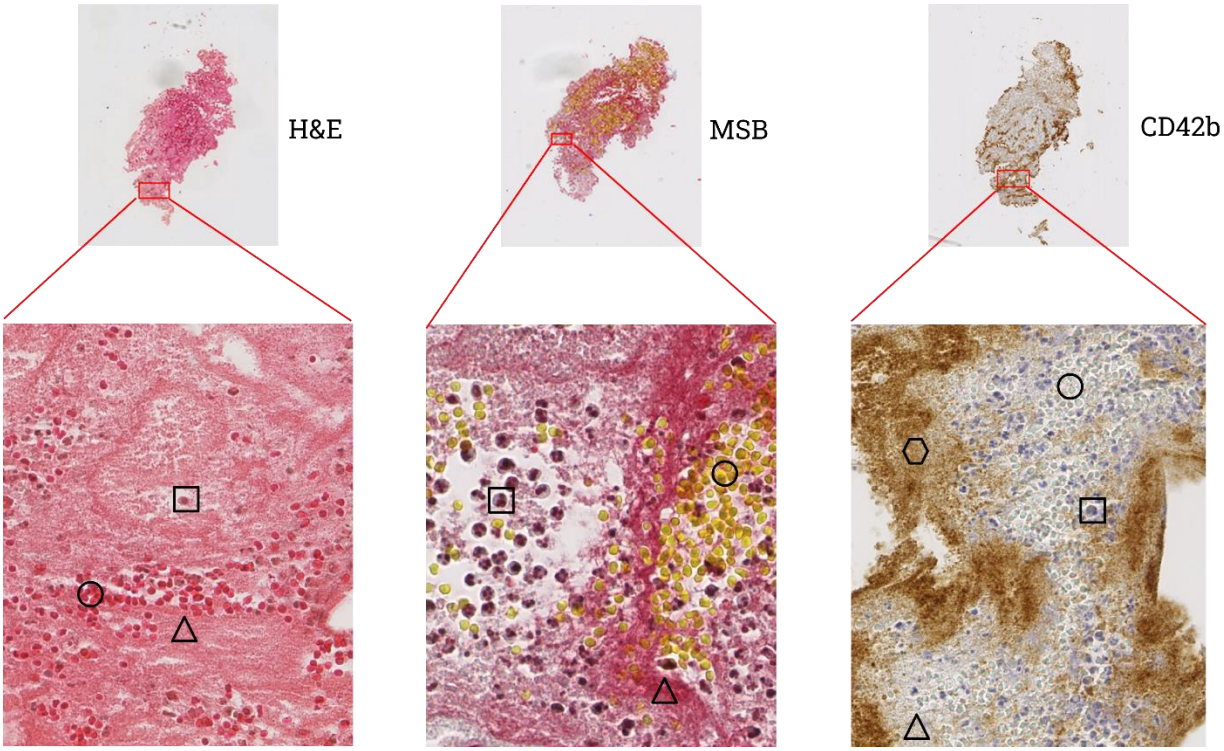

Figure 3: Thrombus components from one mechanical sample stained for H&E, MSB and CD42b; Fibrin marked with triangle, RBC marked with circle, WBC marked with square, and platelets marked with hexagon.

2.6. Statistical analysis

Categorical variables are presented as absolute number and percentage in each group (n, %), while other values are presented as median and interquartile range (IQR) or mean value. Correlations between two continuous variables were evaluated using Pearson and Spearman coefficient analysis, where $p < 0.05$ was considered statistically significant.

Linear regression was applied for fibrin/platelets and RBC to compare the MSB and H&E quantification. The agreement between the two stains was checked by using the Bland-Alman test, with 95% confidence interval. Coefficient of variance was calculated by using standard error and mean values. The Shapiro-Wilk test was used to check if variables follow a normal distribution, and D'Agostino-Pearson test to check for equal variance. The significant difference between groups was determined by using Kruskal–Wallis test, together with Dunn post-hoc test with adjusted Bonferroni alpha level for multiple comparison.

The relationship between thrombi composition and stiffness was analyzed by using linear or piecewise regression models, with 95% confidence and prediction intervals. The inflection points were chosen depending on the overall distribution of stiffness in report to fibrin/platelets, RBC, and platelets composition. Chow test was performed for every piecewise regression to check if the coefficient between two groups was equal, and if there was a structural break (F>F critic) in the data. In addition, a residual analysis was done for every linear regression fit to the data, to check any deviations from linearity, constant variance of residuals, and normal distribution. All statistical analysis was performed by using Microsoft Excel "Real statistics" extension and custom MATLAB scripts.

Table 1: Baseline characteristics of the 20 patients.

Age	median, IQR	76	36-91
Women sex	n, %	17	85
NIHSS score at admission (*n=19)	median, IQR	16	7-24
Time to treatment in minutes	median, IQR	154	80-405
Duration of EVT in minutes (*n=12)	median, IQR	38	24-151
Nr. of passes	median, IQR	2	1-5
Target occlusion location			
ICA	n, %	4	20
M1	n, %	11	55
M2	n, %	5	25
Final TICI score			
2b	n, %	4	20
2c	n, %	4	20
3	n, %	10	50
mRS score	Median, IQR	3	0-6

ICA internal carotid artery, NIHSS National Institutes of Health Stroke Scale. TICI Thrombolysis in Cerebral Infraction, mRS modified Rankin Scale.
*The parameter has only been reported for the indicated number of patients.

3. Results

3.1. Patients clinical and interventional data

Only 20 of the 60 patients who participated in the clinical trial were examined in this study. Table 1 shows the clinical baseline and interventional features for all patients. The patients' median age was 76 years (IQR, 36-91), and 17 (85%) were female. The median National Institutes of Health Stroke Scale (NIHSS) score at admission was 16 (IQR, 7-24). The M1 segment of the middle cerebral artery was the most often occluded site (n=11, 55%), followed by the M2 segment (n=5, 25%) and the internal carotid artery (ICA) terminus (n=4, 20%). 25% of patients experienced thrombus migration to a new region during the MT treatment. The median duration of the EVT procedure was 38 minutes (IQR, 24–151), with a median of 2 passes per patient (IQR, 1–5). Successful reperfusion (TICI 2b/2c/3) was achieved in 90% of the patients.

Of the 20 patients included in the study, one had no appropriate thrombus fragments for mechanical testing, hence only compositional analysis was performed on this patient. An average of 3(IQR, 1-18) thrombus fragments were extracted from each patient, and 4 (IQR, 0-23) cut samples from these fragments were mechanically evaluated under compression. Annex A4 has comprehensive data on all 20 patients.

3.2. Thrombi composition

A total of 249 samples -including mechanical samples, offcuts, and extra parts- were stained for histology. Based on the visual inspection, the retrieved thrombi fragments varied in shape and structure (Figure 1a). The internal structure was highly heterogenous, featuring both well-defined areas and amorphous zones (Figure 3).

The mean composition obtained from H&E staining was 71% (IQR, 14.9-99.7) fibrin/platelet and 29% (IQR, 0.25-85.07) RBC. The mean fibrin/platelet content and RBC content on MSB staining was 65% (IQR, 5.9-99.4) and 35% (IQR, 0.6-94.1), respectively. The median platelet concentration, as determined by CD42b chemical immunostaining, was 43% (IQR, 0-97). Figure C3.1. (Annex C) shows 5 samples with various compositions of RBC.

A detailed analysis of the MSB and CD42b quantification of fibrin/platelets, RBC, and platelets shows the heterogenous composition of the retrieved thrombi in this study. Figure 4 illustrates the results of 229 samples, the rest of 20 samples being excluded due

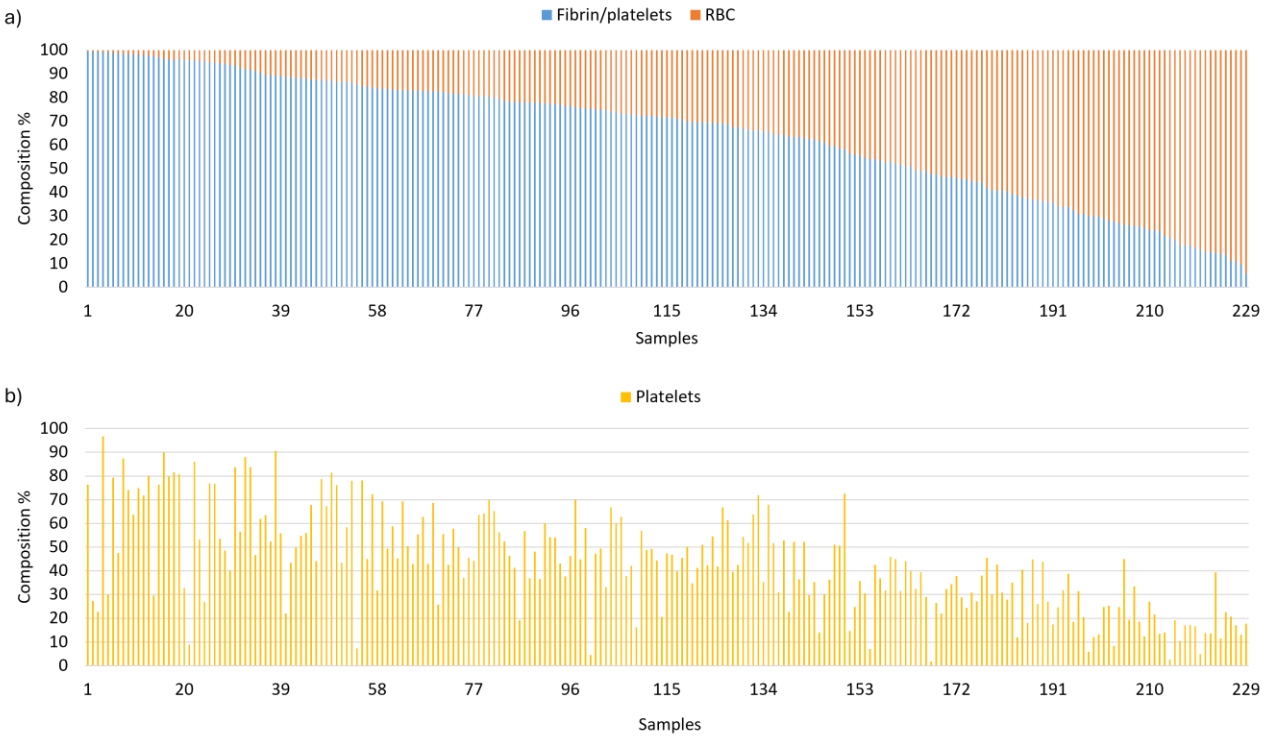

Figure 4: Graphical representation of quantified composition of samples. a) Fibrin/platelets (blue) and RBC (orange) from MSB staining; b)Platelets from CD42b immunostaining.

to incomplete or inaccurate quantification. A wide variation in fibrin/platelets and RBC can be observed. The platelets composition is relatively consistent with and within the fibrin/platelet quantification, with few samples exceeding those values.

The Pearson correlation analysis showed statistically significant relationships between the thrombus components. Fibrin/platelets and RBC had an inverse proportional correlation ($r=-1$, $p=0$), fibrin/platelets and platelets had a moderate positive correlation ($r=0.68$, $p<0.01$), and RBC and platelets had a moderate negative correlation ($r=-0.68$, $p<0.01$). The Spearman analysis results were similar, showing a linear and monotonic relationship between components.

3.2.1. Comparison between MSB and H&E results

Given the observed differences in mean composition values for fibrin/platelets and RBC between MSB and H&E quantifications, a detailed comparison of these methods was performed. Only the samples that had fibrin/platelets and RBC successfully determined for both stains were included. Out of 249 samples, 31 were excluded from this comparison due to missing quantification of one or more elements on H&E and MSB images.

Figure 5 shows a linear regression analysis for fibrin/platelets and RBC concentration values for the two stains. Both fibrin/platelets ($r=0.93$, $p<0.001$) and RBC ($r=0.92$, $p<0.001$) comparisons had a positive linear relationship, with data points distributed around the regression line and a few outliers. The residual analysis (Annex C, Figure C4) showed no obvious deviations from the normal distribution, confirming no systematic errors or non-linearity.

A Bland-Altman analysis (Annex C, Figure C5) was conducted to evaluate the agreement between the two staining methods. For both fibrin/platelets and RBC measurements the mean difference lines were close to zero, indicating minimal systematic bias between MSB and H&E. For fibrin/platelets the MSB measurements had a difference of approximately 5.7 % points lower than on H&E, while for RBC, the MSB measurements had a mean difference on average 5.5 % points higher than H&E.

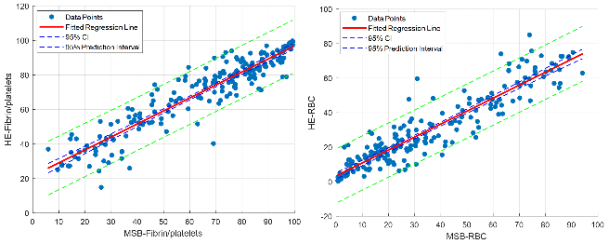

Figure 5: MSB and H&E comparison for fibrin/platelets (left) and RBC (right); linear regression with 95% confidence and prediction interval lines.

The standard deviation of differences indicated moderate variability between the methods, with quantifications measurements differing by up to ~10 % points from the mean difference.

3.2.3. Per patient composition

Per patient composition was calculated using the results from MSB and CD42b. The average composition percentage of all the samples from one patient were calculated. Figure 6 shows the heterogeneity across the 20 patients. Each patient had a different composition. Some cases, like patient 10 exhibited a high percentage of RBC (69.07% RBC), while others, like patient 16, exhibited high levels of fibrin/platelets (94.56%).

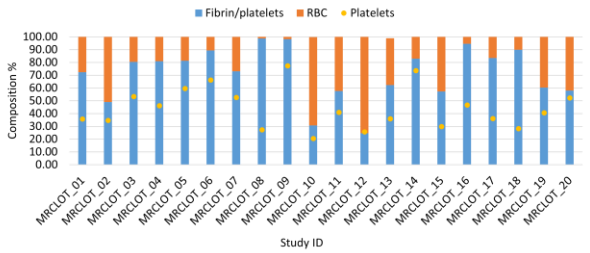

Figure 6: Per patient composition of fibrin/platelets and RBC from MSB, and platelets from CD42b.

Significant intra- and inter-patient variance was found in the histological composition quantification. The inter-patient coefficient of variance (CoV) for RBC (73%) was higher than the CoV for platelets (36.3%), and the CoV for fibrin/platelets (29.4%). The intra-patient variability followed a similar trend, where RBC had the highest CoV (51 %, IQR, 17.2-156.8%), followed by platelets (31%, IQR, 8-77.4%), and fibrin/platelets (21 %, IQR, 0.3-64.5 %). For both inter- and intra-patient CoV, the RBC composition varied greatly, while fibrin/platelets and platelets had a more consistent variation.

3.2.4. Per pass composition

During the EVT procedure, for all the 20 patients included in this study, a number of 47 passes were attempted to retrieve the occluding thrombus. 34 passes (72.3%) were effective in recovering tissue. On the other hand, 13 passes (27.7%) were unsuccessful in obtaining any thrombus fragments and the immediate passes after the failed attempt had a mean composition of 69% fibrin/platelets, 31% RBC, and 41% platelets. A total of 108 thrombus fragments were retrieved from which 5 had incomplete quantification of composition. Per pass analysis is shown in Figure 7. The mean fibrin/platelets composition for each pass was 61%, 75%, 70%, 73%, and 83% respectively.

The Kruskal-Wallis's test for fibrin/platelets found no statistically significant difference between the individual passes (p=0.053), which was confirmed by the Dunn post hoc test (p> 0.005). When passes were grouped, however, significant differences were found between pass 1 and the combined group of passes 2, 3, 4, and 5, as well as between passes 1 and 2 compared to passes 3, 4, and 5 together.

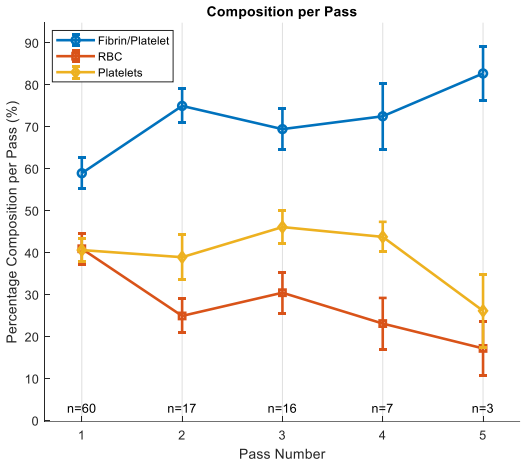

Figure 7: Mean fibrin/platelet, RBC, and platelets composition from n number of thrombi fragments retrieved in each pass.

The mean RBC composition per pass was 39%, 25%, 31%, 23%, and 17% respectively. For RBC the Kruskal-Wallis test indicated differences between single passes (p=0.041), but the post-hoc test did not find any significant difference between any two passes. When passes were grouped, significant differences were seen between pass 1 and the other passes combined (p<0.05), as well as between pass 1 and 2 compared with passes 3,4, and 5 together (p<0.05).

The mean platelet composition per pass was 44%, 39%, 46%, 44%, 26%. For platelets, neither the Kruskal-Wallis test nor Dunn test found any significant differences, whether comparing individual or grouped passes.

3.3. Mechanical properties

A total of 138 samples were tested under compression, from which 11 samples were excluded for various reasons detailed in Annex B1. In addition, one patient did not have any suitable retrieved thrombus fragments that could be used for mechanical testing.

Figure 8 shows the low (E_{10}) and high (E_{75}) strain stiffness of each sample for each patient. The median thrombus stiffness for E_{10} was 1.76 (IQR, 0-48) kPa. In Figure 8a it can be observed that 96.8% of samples had a E_{10} values under 10kPa. The overall analysis identified 4 samples as outliers, such as patient 8 where E_{10} was

over 40kPa. Inter-patient low stiffness CoV reached 193%, while intra-patient CoV had a mean value of 78% (IQR, 13.4-124%).

The high strain stiffness (Figure 8b) had a median value of 576.4 (IQR, 47-1679) kPa. No outliers were identified in the overall analysis. For patients with more than two samples, various E_{75} ranges were observed; for example, for patient 15 E_{75} had a range from 47 kPa to 162 kPa, while patient 7 had E_{75} values that ranges between 390 kPa to 1453 kPa. Inter-patient CoV for high strain stiffness was 61%, while mean intra-patient CoV was 78% (IQR, 6.7-60.5%).

A significant correlation between E_{10} and E_{75} ($r=0.33$, $\rho=0.51$, $p<0.01$) was found. The T-test showed that E_{10} is significantly lower than E_{75} ($p<0.01$) with a magnitude of 634 kPa, and a large effect size (Cohen's $d=1.64$). Figure 8c shows individual stress-strain curves of the first cycle of all samples from patient 3. All thrombus samples exhibited nonlinear mechanical behavior and stain stiffening at higher stains. Over the 20 cycles all samples presented a reduction in peak stress, exhibiting a softening effect.

The nonlinearity of the thrombus samples was also confirmed by the hysteresis loading and unloading curves. Figure 8d shows how the hysteresis area was decreasing in size as the cycle number increased, an indicative of energy dissipation over time. After the first cycle there was a noticeable decrease in hysteresis area, meaning that the samples were not getting back to their original state. For most of the samples the hysteresis formed an overlapping area at the top of the curve, immediately after the loading phase stopped and the unloading began. The mean hysteresis area (HysA) was 1.6 (IQR, 0.06-13) kPa, and the hysteresis ratio (Hys R) was 37 (IQR, 20.8-83.3) %. Between the two variables there was a weak negative linear relationship ($r=-0.25$, $p<0.01$). The softening behavior in time, the non-linearity of the stress strain curves, and the hysteresis, are clear features of viscoelastic behavior.

Table 1: Mean values of low and high strain stiffness, hysteresis area, and hysteresis ration.

	Pass 1	Pass 2	Pass 3	Pass 4	Pass 5
E10 (kPa)	3.45	2.28	2.08	0.38	3.56
E75 (kPa)	640.70	470.61	736.48	395.20	661.10
Hys A (kPa)	1.8	0.5	15	0.6	18
Hys R (%)	37.51	43.79	33.51	30.26	32.27

A per pass analysis of the mechanical properties is presented in Table 2. 66.9% of the mechanical samples came from Pass 1, 19.7% samples from Pass 3, 11% from Pass 2, and 2.4% from Pass 4 and 5 combined. It can be observed that the pass number to which a sample belonged did not influence the mechanical properties in any way and no trend was established.

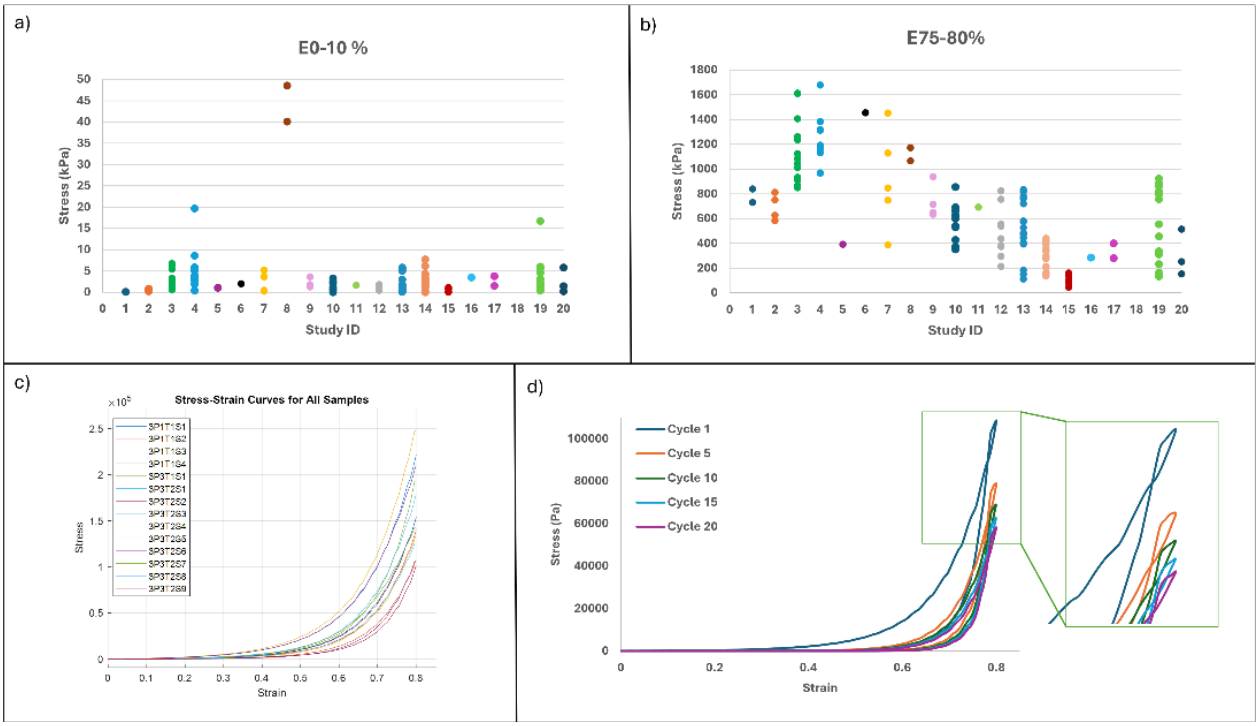

Figure 8: Mechanical properties and non-linear behavior of thrombus samples: low strain (a) and high strain (b) stiffness calculated as mean value per patient; c) Stress-strain curves of 14 samples from patient 3; d) hysteresis curves from 5 to 5 cycles.

The Kruskal-Wallis test showed no significant difference in stiffness between all passes ($p>0.005$), which was confirmed by the post hoc analysis for both single paired or grouped paired passes. Regarding the hysteresis area, the single paired analysis showed significant differences between pass 2 and pass 3 ($p<0.01$) and pass 2 and 5 ($p<0.05$). In grouped analysis a few other significant differences were revealed: pass 1 and 2 ($p<0.01$); pass 2 and 3 ($p<0.01$); pass 2 and pass 3, 4, and 5 combined ($p<0.01$). For the hysteresis ratio, the first 3 passes were significantly different in single paired analysis. The first two passes combined were different compared with pass 3 ($p<0.01$), and compared with pass 3, 4, and 5 together ($p<0.01$).

3.4. Composition in relation to mechanical properties

Linear regression models revealed complex relationships between composition and mechanical properties. A general trend was observed, where the mechanical properties were changing at different concentrations of fibrin/platelets, RBC, and platelets. Inflection points were noticed in the overall distribution of stiffness and hysteresis area in relation to composition. These specific points were used to model the piecewise linear regression. Residual analysis indicated no obvious deviations from linearity or heteroscedasticity (unequal variance) for any segment of data, but small deviations from the normal distribution and a few outliers were found.

Between fibrin/platelets and E_{75} (Figure 9a) there was a positive significant correlation ($r=0.3$, $p<0.01$). A wide range of E_{75} can be observed for any given fibrin/platelets %, and an even greater increase in variability for values >70% fibrin/platelets. The Chow test showed no significant difference in the data at the 70% composition inflection point.

For low strain stiffness the Chow test revealed a structural break at 60% and 80% fibrin/platelets. In Figure 9b it can be observed that E_{10} remains constant prior to 60% fibrin/platelets, increases from 60% to 80% fibrin/platelets, and then tends to decrease after 80%. For all segments, there was no statistically significant association ($r<0.5$, $p>0.05$) between low strain stiffness and fibrin/platelets.

A similar trend was followed by the hysteresis area in relation to fibrin/platelets concentration (Figure 9c). However, no significant correlations ($r<0.5$, $p>0.05$)

.

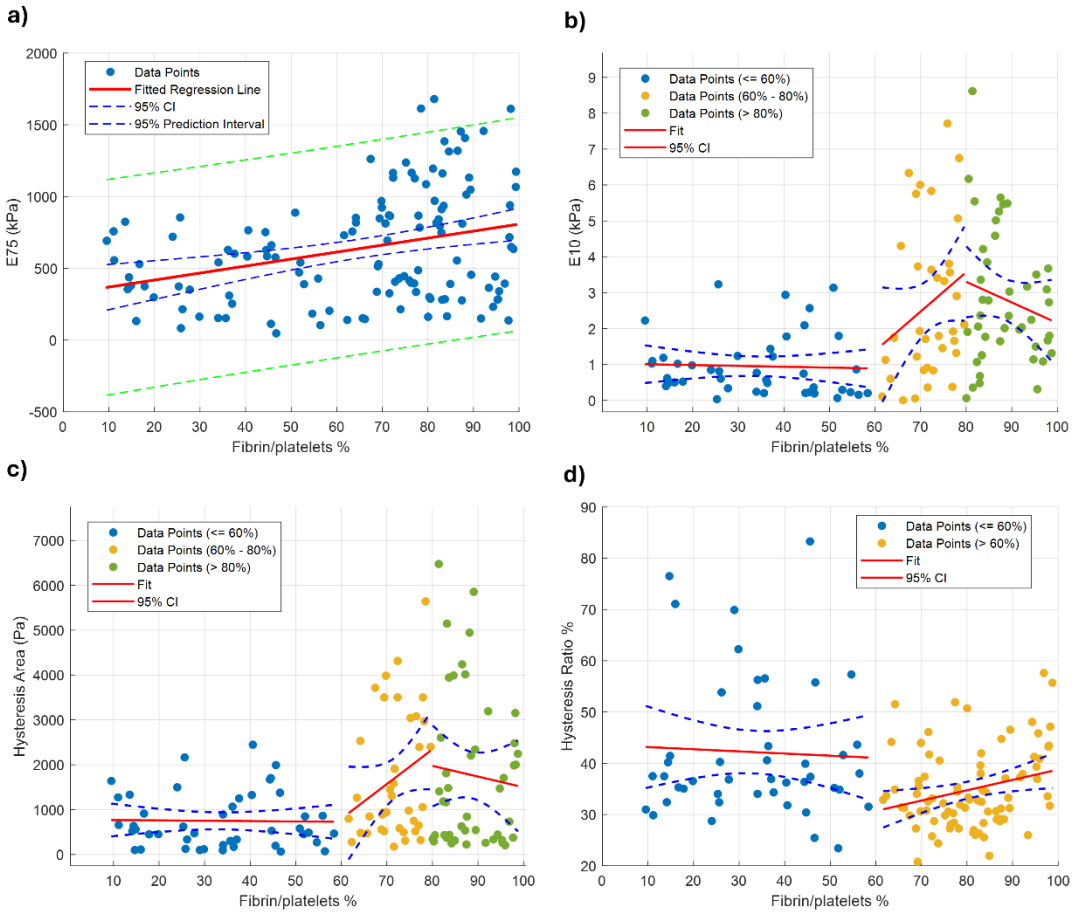

Figure 9: Relationship of fibrin/platelets composition with E75 (a), E10 (b), hysteresis area (c), and hysteresis ratio (d). Plots include 95% confidence interval.

was found for any of the segments divided by the 60% and 80% fibrin/ platelets inflection points.

The hysteresis ratio changed at 60% fibrin/ platelets (Figure 9d). Until 60% fibrin/platelets there was a weak negative correlation (r=-0.05, p>0.05), followed by a positive significant correlation from 60% to 100% fibrin/platelets (r=0.26, p<0.05).

Figure 10a illustrates the wide variation of E_{75} in relation to RBC composition. A significant negative correlation (r=-0.3, p<0.01) was established between the two. No distinctive RBC composition was found to influence the high strain stiffness.

On the other hand, the low strain stiffness changed with the RBC concentration. Figure 10b illustrates how E_{10} increases from 0% to 20% RBC, decreases from 20-60% RBC, and increases slightly after 60% RBC. The Chow test confirmed the breakpoints. The second segment, 20-60% RBC had a significant correlation with E_{10} (r=-0.39, p<0.01).

The hysteresis area follows the same trend as E_{10} (Figure 10c), with two significant breakpoints at 20% and 40% RBC, but no significant correlations for any of the segments (r<0.5, p>0.05) were found. Figure 10d shows the relation between hysteresis ratio and RBC %. The hysteresis ratio had a negative trend from 0% to 40% RBC (r=-0.26, p<0.05), followed by a slight increase after 40% RBC (r=0.05, p>0.05).

E_{10} and E_{75} increased with the increase in platelets concentration up to 60% platelets, followed by a decrease up to 90% platelets (Figure 11a and b). The Chow test confirmed the inflection point. Although there was a large distribution range of E_{75} before 60% platelets, a significant correlation (r=0.43, p<0.01) between the two was found. Similarly, E_{10} had a positive correlation with platelets before 60% (r=0.39, p<0.01).

Figure 11c shows how the hysteresis area followed the same trends as the stiffness, with a significant correlation with platelets (r=0.43, p<0.01) before the breaking point at 60% platelet content, and a very weak correlation after that (r=-0.06, p>0.05). The hysteresis ratio, illustrated in Figure 11d, decreased from 0% to 40% platelets (r=-0.28, p<0.05) and increases from 40% to 90% platelets (r=0.15, p>0.05).

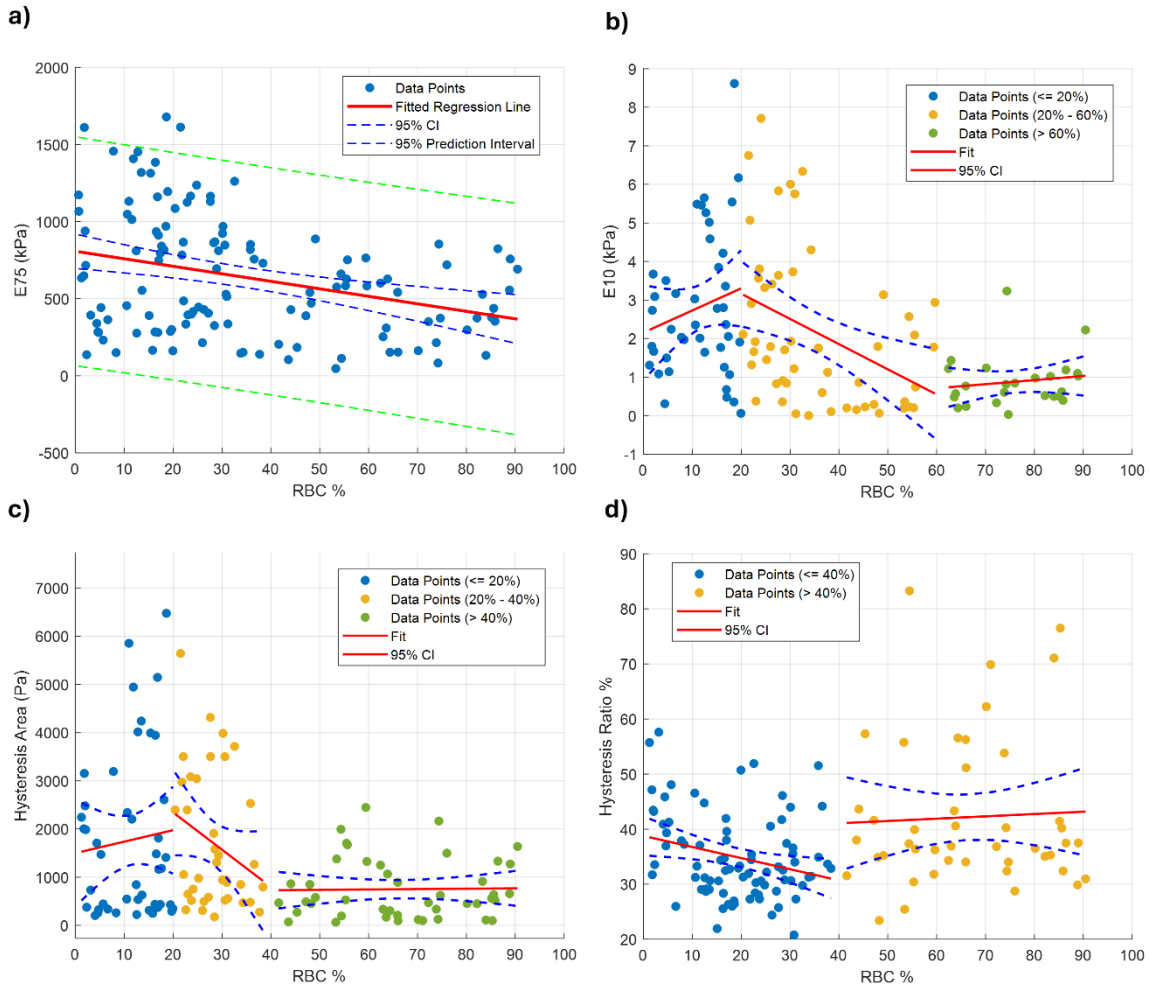

Figure 10: Relationship of RBC composition with E75 (a), E10 (b), hysteresis area (c), and hysteresis ratio (d). Plots include 95% confidence interval.

4. Discussion

Understanding the composition and mechanical properties of AIS thrombi is crucial for optimizing EVT procedures for acute ischemic stroke. While many studies have histologically evaluated thrombus composition [11] [12] [13], few provide detailed per-pass analyses of AIS thrombi [14] [15] [16]. Though laborious and time-consuming, per-pass analysis can provide more insights into why successful recanalization is achieved in only 70% to 80% of cases [14]. Moreover, scarce knowledge exists on the ex vivo mechanical characteristics of stoke thrombi, with only three relevant articles published in the last 10 years [5] [3] [4]. These highlight the necessity of bridging the gap between physical properties and composition, which can optimize device selection during MT and enhance treatment success rates. In this study, ex vivo thrombi composition and mechanical properties under compression were quantitatively determined.

Thrombus morphology revealed a variety of different thrombi compositions such that every sample was histologically unique. The fibrin/platelet and RBC composition spanned a wide range. The complex interplay between the components of thrombi was highlighted by the substantial correlation between fibrin/platelets, RBC, and platelets. This is indicative of the in vivo thrombus formation when diverse structural areas are developed [18] [13]. In addition, RBC exhibited the highest inter-patient variability, followed by more moderate discrepancies in fibrin/platelet and platelet contents. RBC content also had the largest variability within patients, demonstrating that RBC composition can vary substantially within a single patient. The overall findings are in line with previous research, confirming the significant heterogeneous nature of thrombus composition between and within patients [15] [9].

The comparison between MSB and H&E showed minor measurement disagreements, as indicated by the small mean biases and systematic differences. This could be due to the subjectivity of the Orbit to the quality of the H&E tissue staining used in this investigation, which had similar colors and intensity for

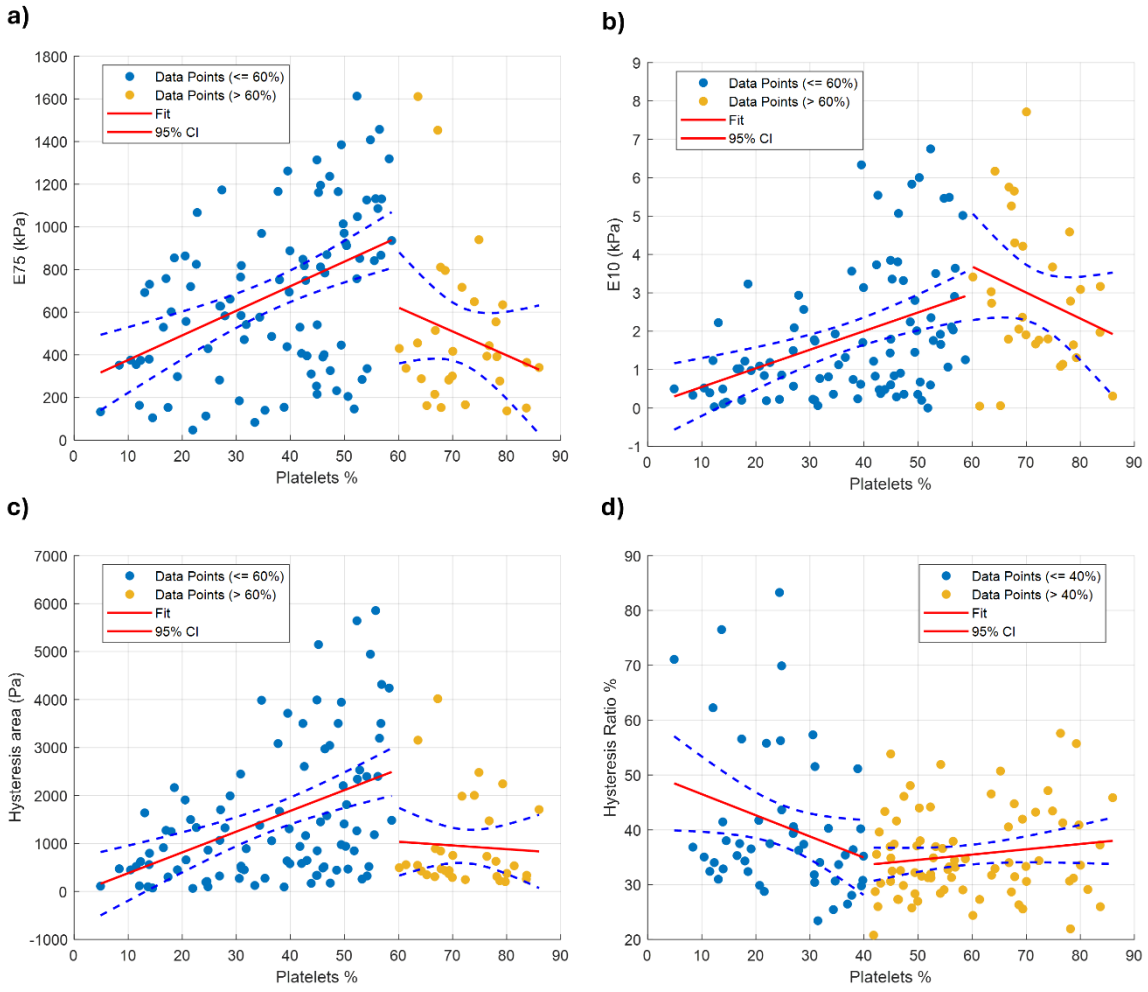

Figure 11: Relationship of Platelets composition with E75 (a), E10 (b), hysteresis area (c), and hysteresis ratio (d). Plots include 95% confidence interval.

distinct thrombus components. This is known as a primary problem of digital pathological analysis, which can be overcome by using an Autostainer rather than individual researchers [8]. Nevertheless, the quantification of MSB and H&E were fairly in good agreement; fibrin/platelet readings on MSB were often lower and RBC% readings greater than on H&E. Duffy et al. confirmed a similar agreement with no significant differences between the two stains, despite using manual quantification method [19]. Therefore, both staining methods can be used for qualitative assessment of composition, but MSB should be preferred over H&E due to the high contrast between structural components.

A high number of passes were successful in retrieving thrombus tissue (72.3%), which is comparable to rates reported in other studies, such as 76.8% for Duffy et al. [14] and 72% for Fitzgerald et al. [16]. Research suggests that the chances of successfully retrieving RBC-rich thrombi are highest on the first pass [12], or during the first two passes [20] [21], with no discernible RBC composition difference between the two [15]. This is consistent with the first pass data obtained here, which showed a significantly higher RBC composition (39%). Furthermore, it was discovered that thrombus pieces recovered during the initial pass had a larger extracted tissue area [16], which is confirmed in our study by the high amount of thrombus fragments (n=60) that were retrieved, resulting in a high percentage of mechanical samples (66.7%).

Fibrin/platelets concentrations increased with the number of passes. Compared to the mean fibrin values reported for pass 4 by Fitzgerald et al. [16] (38.0%) and by Abassi et al. [15] (32.6 %), the maximum of 83% fibrin/platelets found in this study in pass 5 was significantly higher. It must be noted that the later passes (pass 4 and 5) in the current work produced a small number of samples which might have led to less relevant results than the ones found in the literature. Nevertheless, the association between fibrin/platelets and later passes remains unchanged, as pass one had significantly reduced fibrin/platelet composition.

In terms of platelets, pass 3 had the highest composition (46%), exceeding the maximum found by Abassi et al. in pass 4 (30.5%) [15]. In contrast with the previous findings, that state the platelets concentration is increasing with the number of passes, this study found no connection between the two [16]. The immediate passes following a failed attempt had high levels of fibrin/platelets (69%) and platelets (41%), which shows their overall contribution to thrombus resistance removal, leading to longer procedure times and worse angiographic outcomes [15] [21].

The mechanical properties of human AIS thrombi were also assessed. The low strain stiffness under unconfined compression had a median of 1.76 (IQR, 0-48) kPa, with E_{10} lower than 10 kPa in 96.8% of the samples. The limited research on low strain stiffness in real thrombi calls for comparisons with human blood clot analogs. The E_{10} median value obtained here is within the E_{10} range (~0.1-7.5 kPa) reported by Cahalane et al. [22] for clots with 0% to 80% RBC volume. This indicates that at low strains, both clot analogs and real thrombi exhibit a low stress due to their very soft nature. Juega et al.[5] showed that ex vivo stroke thrombi exhibit a median of 30.2 kPa (IQR, 18.9-42.7) at slightly higher strains (0-45%). Comparing the median values, the stiffness seems to increase with strain, while the variability seems to decrease.

E_{10} had a non-linear relationship with the RBC, following the same pattern as the clot analogs investigated by Cahalane et al. [22]. In addition, E_{10} was favorably correlated with the increase in platelet levels up to 60%, however there was no significant association with the composition of fibrin/platelets, despite the 2 inflection points found.

All mechanical samples exhibited non-linear hyperelastic behavior and significant strain stiffening at higher strains. Under compression, this behavior can be attributed to fibrin fiber densification and the RBC resistance to deformation within the network [22] [23]. The high strain stiffness (E_{75}) had a median of 576.4 (IQR 47-1679) kPa, consistent with previous AIS thrombi results (393-1161 kPa) reported by Boodt et al. [3]. Furthermore, the results also fall within the ultimate stress range recorded by Liu et al. under tensile failure tests (63-2396 kPa) for real thrombus [4].

Fibrin/platelets and RBC had a weak linear relationship with E_{75}, contrary to the much stronger relationship found by Boodt et al. [3], where for each 1% increase in fibrin/platelets a 9 kPa increase in stiffness was noticed. The platelet concentration from 0% to 60% increased the high strain stiffness. Beyond 60% platelets the stiffness seemed to decrease, which is in contrast to the increasing trend found by Boodt et al. after 70% platelets. These disparities across studies call for additional investigation, possibly involving the use of more sophisticated regression models, to comprehend the underlying interplay between E_{75} and composition.

The findings by Boodt et al. [3] and Liu et al. [4] show the stiffer nature of fibrin/platelet rich thrombi

which increases resistance to compressive forces and can impede the grip and indentation depth of the stent retrieval, hindering successful recanalization [24].

Between low strain and high strain stiffness, there was a high correlation, with 634 kPa magnitude difference between mean values. The inter-patient variability for E_{10} was exceptionally high, at 193%, whereas for E_{75} it was 61%. In contrast, the maximum inter-donor CoV values reported by Cahalane et al. [22] for blood clot analogs were lower for E_{10} (75%), but very similar for E_{75} (69%). The intra-patient mean CoV in the current study was 78% for both E_{10} and E_{75}, while Cahalane et al. obtained a CoV of maximum 47% for E_{10} and 30% for E_{75}. Compared with the present study, Cahalane et al. had a small number of samples, used static formation, and different hematocrit levels, which may not fully represent real stroke thrombi composition. In addition, the authors anticipated a greater inter- and intra-patient variability in real AIS thrombi, which aligns with the findings of this study. To my knowledge, no previous research has reported inter- and intra-patient CoV for stroke thrombi.

No correlation was made between pass numbers and E_{10} and E_{75}. The highest mean E_{10} was found in pass 5, while the highest mean E_{75} values were found in pass 3 (736.48 kPa) and pass 5 (661.10 kPa). This emphasizes that later passes had thrombus fragments with increased stiffness, potentially hindering the recanalization process during thrombectomy procedure.

Compression loading and unloading did not follow the same pathway, resulting in hysteresis due to energy dissipation. For all samples, the amount of hysteresis decreased with each cycle, with a noticeable drop after the first cycle. This suggests that samples do not return to their initial state before compression, losing more energy during the loading period than recovering it during the unloading phase. The mean hysteresis area was 1.6 kPa, and the mean hysteresis ratio was 37% (IQR, 20.8-83.3%). Liang et al., on the other hand, found that the hysteresis area for human blood analogs was above the results found here, ranging from 2.21 kPa to 5.52 kPa [25]. The structural differences between in vivo thrombi and analog clots, together with the various compressive strain rates used by the authors, explain the difference in results.

Given the fact that the overlapping loop at the top of the hysteresis curves was consistent across all samples, the occurrence cannot be caused by an error in the testing setup or by experimental execution. A more likely explanation can be found inside the thrombus samples structure. During compression, RBC can migrate from dense to less dense regions; however, during loading and unloading, they can also migrate out of the sample along with interstitial fluid and be drawn back in. Moreover, the fibrin fiber can reorient and compact closer together within the matrix, forming bundles that enhance the local stiffness. All these microstructural changes dissipate energy that is reflected in the hysteresis curves.

The hysteresis area had no significant correlation with fibrin/platelets, however there was an increase between 60% and 80% fibrin/platelets, followed by a decrease after 80%. In terms of RBC, the hysteresis area increased up to 20% RBC, then decreased up to 40% RBC. Platelets were significantly correlated with an increase in hysteresis area up to 60% platelets. The hysteresis ratio had a high variability from 10% to 60% fibrin/platelets, with a significant increasing trend after 60%. A significant correlation was found between hysteresis ratio and RBC, with a decrease from 0% to 40%, followed by a high variability after that point. Platelets were significantly correlated with a decrease in hysteresis ratio up to 40% platelets.

In conclusion, the composition of thrombi plays a pivotal role in determining their mechanical behavior during thrombectomy procedures and may serve as an indicator for predicting the recanalization rate and the ultimate outcome of the operation [26]. A one-size-fits-all strategy is unsuitable for acute ischemic stroke thrombi, which can have a wide range of compositions and mechanical properties, as demonstrated in this study.

5. Limitations

This study has certain limitations that should be noted. The patient population size was relatively small, as is part of a much larger clinical study. Despite this, the high number of histological and mechanical samples was considered comparable with current literature research and representative of a diverse variety of in vivo thrombi. The retrieved thrombi had multiple fragments, where extra and offcut samples were not used for compression testing, potentially introducing a bias.

The unconfined compression test is a basic testing approach; however, it does not capture the whole mechanical behavior of thrombi that are subjected to multi-axial loading at varying strain rates during retrieval. Furthermore, thrombus characteristics and composition may have changed during retrieval and

mechanical testing, therefore the results may not reflect the original in vivo thrombus features.

The histology analysis was done by a single observer which might have influenced the composition quantification. The histology was also limited by the H&E staining slides that in some cases had an inadequate distinction between pink and red hues. Platelets were quantified separately on a CD42b immunostaining, and the proportion occasionally exceeded the fibrin/platelets % on MSB and H&E staining. Moreover, WBCs were not measured in this study. Although WBCs are present in small amounts in AIS thrombi, they do contribute to thrombus resistance by increasing thrombus stiffness and adhesion to the artery wall [11] [5].

For the mechanical samples subjected to 60% stain rate the stress-strain curves were extrapolated using a Gaussian regression model which allows for similar non-linear curves as the original stress-strain curve at 80% compression. Nevertheless, a computational viscoelastic model would be more appropriate to extrapolate such data.

6. Conclusion

This study characterized the composition and mechanical properties of AIS thrombi using a per pass approach. Significant variation in composition and mechanical stiffness was found both between and within patients. A lower fibrin/platelet content and a greater RBC content was correlated with the first pass. Under compression thrombi samples exhibited a non-linear behavior, where stress is highly dependable on strain. While low strain stiffness, hysteresis area, and ratio changed with varying quantities of fibrin/ platelets, RBC, and platelets composition, the high strain stiffness exhibited a linear correlation with fibrin/platelets and RBC. Future research should incorporate detailed per-pass compositional and mechanical characterization, as well as preoperative imaging and angiographic outcomes, under the power of digital twinning that can enable personalized treatment for the best functional outcome of patients.

7. References

[1] V. Feigin, M. Brainin, B. Norrving and e. al., "World Stroke Organization (WSO): Global Stroke Fact Sheet 2022," International Journal of Stroke, vol. 17, no. 1, pp. 18-29, 2022.

[2] J. Kleine, S. Wunderlich, C. Zimmer and J. Kaesmacher, "Time to redefine success? TICI 3 versus TICI 2b recanalization in middle cerebral artery occlusion treated with thrombectomy," Journal of neurointerventional surgery, vol. 9, no. 2, pp. 117-121, 2017.

[3] N. Boodt, P. R. Snouckaert Van Schauburg, H. M. Hund, B. Fereidoonnezhad, J. P. McGarry, A. C. Akyildiz, A. C. Van Es, A. Van Der Lugt and F. J. Gijsen, "Mechanical Characterization of Thrombi Retrieved with Endovascular Thrombectomy in Patients with Acute Ischemic Stroke," Stroke, vol. 52, no. 8, pp. 2510-2517, 2021.

[4] Y. Liu, Y. Zheng, A. S. Reddy, D. Gebrezgiabhier, E. Davis, J. Cockrum, J. J. Gemmete and e. al., "Analysis of human emboli and thrombectomy forces in large-vessel occlusion," Journal of Neurosurgery, vol. 134, no. 3, pp. 893-901, 2020.

[5] J. Juega, J. Li, C. Palacio-Garcia, M. Rodriguez, R. Tiberi, C. Piñana, D. Rodriguez-Luna, M. Requena and e. al., "Granulocytes-Rich Thrombi in Cerebral Large Vessel Occlusion Are Associated with Increased Stiffness and Poorer Revascularization Outcomes," Neurotherapeutics, vol. 20, no. 4, pp. 1167-1176, 2023.

[6] R. Cahalane, N. Boodt, A. Akyildiz and e. al., "A review on the association of thrombus composition with mechanical and radiological imaging characteristics in acute ischemic stroke," Journal of Biomechanics, vol. 129, p. 110816, 2021.

[7] S. M. R. G. M. e. a. Johnson, "Investigating the Mechanical Behavior of Clot Analogues Through Experimental and Computational Analysis," Ann Biomed Eng, vol. 49, pp. 420-431, 2021.

[8] S. Fitzgerald, S. Wang, D. Dai, M. Jr.D.H., A. Pandit, A. Douglas and e. al., "Orbit image analysis machine learning software can be used for the histological quantification of acute ischemic stroke blood clots.," PlOS one, vol. 14, no. 12, p. e0225841, 2019.

[9] S. Staessens, F. Denorme, O. Francois, L. Desender, T. Dewaele, P. Vanacker, H. Deckmyn, K. Vanhoorelbeke, T. Andersson and S. De Meyer, "Structural analysis of ischemic stroke thrombi: histological indications for therapy resistance," Haematologica, vol. 105, no. 2, pp. 498-507, 2020.

[10] S. Staessens, S. Fitzgerald, T. Andersson, F. Clarençon, F. Denorme, M. Gounis and e. al., "Histological stroke clot analysis after thrombectomy: Technical aspects and recommendations," International Journal of Stroke, vol. 15, no. 5, pp. 467-476, 2020.

[11] T. Boeckh-Behrens, M. Schubert, A. Forschler, S. Prothmann, K. Kreiser and e. al., "The impact of histological clot composition in embolic stroke.," Clin Neuroradiol., vol. 26, pp. 189-197, 2016.

[12] O. M. Mereuta, R. Rossi, A. Douglas, S. M. Gil, S. Fitzgerald, A. Pandit, R. McCarthy, M. Gilvarry, E. Ceder, D. Dunker, A. Nordanstig, P. Redfors, K. Jood, G. Magoufis, K. Psychogios and G. e. a. Tsivgoulis, "Characterization of the 'White' Appearing Clots that Cause Acute Ischemic Stroke," Journal of Stroke and Cerebrovascular Diseases, vol. 30, no. 12, p. 106127, 2021.

[13] Y. Liu, W. Brinjikji, M. Abbasi, D. Dai, J. L. A. Larco, S. I. Madhani, A. H. Shahid and e. al., "Quantification of clot spatial heterogeneity and its impact on

thrombectomy," Journal of NeuroInterventional Surgery, vol. 14, no. 12, pp. 1248-1252, 2022.

[14] S. Duffy, R. McCarthy, M. Farrell, S. Thomas, P. Brennan, S. Power and e. al., "Per-Pass Analysis of Thrombus Composition in Patients With Acute Ischemic Stroke Undergoing Mechanical Thrombectomy," Stroke, vol. 50, no. 5, pp. 1156-1163, 2019.

[15] M. Abbasi, P. Kvamme, K. F. Layton, R. A. Hanel, M. A. Almekhlafi, J. E. Delgado and e. al., "Per-pass analysis of recanalization and good neurological outcome in thrombectomy for stroke: Systematic review and meta-analysis.," Interventional Neuroradiology., vol. 27, no. 6, pp. 815-820, 2021.

[16] S. Fitzgerald, R. Rossi, O. M. Mereuta, D. Jabrah, A. Okolo, A. Douglas, S. M. Gil and e. al., "Per-pass analysis of acute ischemic stroke clots: impact of stroke etiology on extracted clot area and histological composition," Journal of NeuroInterventional Surgery, vol. 13, no. 12, pp. 1111-1116, 2021.

[17] J. W. W. Rustem I. Litvinov, "Blood clot contraction: Mechanisms, pathophysiology, and disease," Research and Practice in Thrombosis and Haemostasis, vol. 7, no. 1, p. 100023, 2023.

[18] S. Duffy, M. Farrell, K. McArdle, J. Thornton and e. al., "Novel methodology to replicate clot analogs with diverse composition in acute ischemic stroke.," Journal of Neur, vol. 9, no. 5, pp. 486-491, 2017.

[19] K. Maekawa, M. Shibata, H. Nakajima and et al., "Erythrocyte-Rich Thrombus Is Associated with Reduced Number of Maneuvers and Procedure Time in Patients with Acute Ischemic Stroke Undergoing Mechanical Thrombectomy," Cerebrovasc Dis Extra, vol. 8, no. 1, pp. 39-49, 2018.

[20] H. Shimizu, K. Hatakeyama, K. Saito, R. Shobatake, N. Takahashi, J. Deguchi and e. al., "Age and composition of the thrombus retrieved by mechanical thrombectomy from patients with acute ischemic stroke are associated with revascularization and clinical outcomes," Thrombosis Research, vol. 219, pp. 60-69, 2022.

[21] R. M. E. Cahalane, J. J. de Vries, M. P. M. de Maat, K. van Gaalen, H. M. van Beusekom and e. al., "Tensile and Compressive Mechanical Behaviour of Human Blood Clot Analogues," Annals of Biomedical Engineering, vol. 51, no. 8, pp. 1759-1768, 2023.

[22] R. Khismatullin, C. Nagaswami, A. Shakirova, A. Vrtková, V. Procházka, J. Gumulec, J. Mačák, R. Litvinov and J. and Weisel, "Quantitative Morphology of Cerebral Thrombi Related to Intravital Contraction and Clinical Features of Ischemic Stroke," Stroke, vol. 51, p. 3640–3650, 2020.

[23] F. Weafer, S. Duffy, I. Machado, G. Gunning, P. Mordasini, E. Roche and e. al., "Characterization of strut indentation during mechanical thrombectomy in acute ischemic stroke clot analogs," Journal of Neurointerventional Surgery, vol. 11, no. 9, pp. 891-897, 2019.

[24] X. Liang, I. Chernysh, P. K. Purohit and J. W. & Weisel, "Phase transitions during compression and decompression of clots from platelet-poor plasma, platelet-rich plasma and whole blood," Acta Biomaterialia, vol. 60, p. 275–290, 2017.

[25] T. Hashimoto, M. Hayakawa, N. Funatsu, H. Yamagami, T. Satow, J. Takahashi, K. Nagatsuka, H. Ishibashi-Ueda, J. Kira and T. K., "Histopathologic Analysis of Retrieved Thrombi Associated With Successful Reperfusion After Acute Stroke Thrombectomy," Stroke, vol. 47, no. 12, pp. 3035-3037, 2016.

[26] S. Staessens and S. De Meyer, "Thrombus heterogeneity in ischemic stroke," Platelets, vol. 32, no. 3, p. 331–339, 2021.

[27] Z. G. M. &. C. N. Wang, "Viscoelastic Properties of Cardiovascular Tissues," IntechOpen, 2016.

A

Collection and preparation of thrombus samples

A1. Collection

During the recruitment period from August 2022 to July 2023, patients underwent consecutive enrollment on weekdays from 8 AM to 6 PM, excluding a two-week interval in December. For each patient receiving Endovascular Thrombectomy for AIS, five containers with DMEM were prepared and stored at 4°C. These were labeled 1-5 to match potential pass numbers used by the interventionalist. Only 5 containers were used to ease the collection process for the intervention team, but also because in literature most cases do not need higher number of passes [16]. Therefore, thrombus material from any pass exceeding five was collected in the fifth container. All the intervention teams were instructed on the thrombi collection procedure and the designated hours. The doctor completed a form at the end of the procedure, recording details such as the number of passes, the device utilized, recanalization scores after each pass, and the final score.

Baseline clinical data of patients were taken out from the internal hospital system of Erasmus MC and stored in a protected database. Written informed consent for mechanical testing and histopathological analysis of the retrieved thrombi was obtained from the patient, or a family member if the patient was incapacitated, following the procedure. The thrombus containers and the intervention form were collected as soon as possible after the procedure. In case of more than 5 min delay in pick up, the containers were stored back at 4°C.

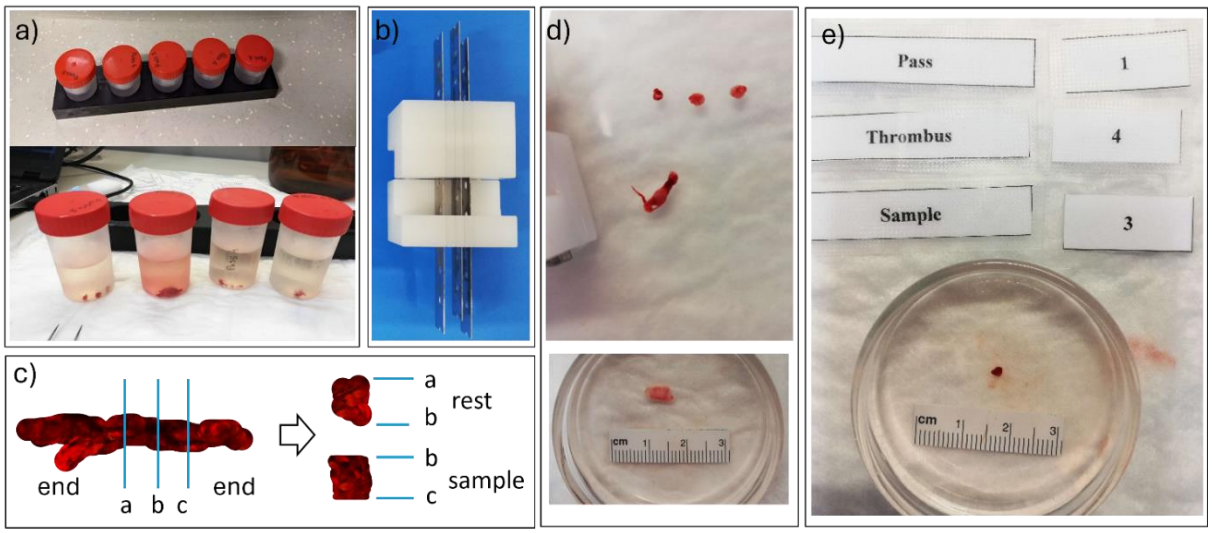

Figure A1: a) Per pass containers with thrombus fragments; b) Cutting mold; c) Thrombi fragment cutting with one sample for mechanical testing and rest and end parts as 'offcut samples'; d) Thrombi fragments examples; e) One mechanical sample.

A2. Preparation

Each fragment from every pass was individually photographed in a Petri dish containing HEPES buffer and a small ruler for scale. Larger fragments were sectioned into 1 mm or 2 mm samples with two flat parallel faces using a cutting mold, as depicted in Figure A1b). The chosen cutting size was dictated by the fragment diameter. If the sample diameter is too small, the contact area with the testing apparatus decreases, which can lead to potential slippage or uneven force application. Conversely, taller samples are prone to buckling or barrelling. To address this, a height-to-diameter aspect ratio of 1.5 (d=1.5*h) was maintained, ensuring uniform stress distribution during compression and thereby enhancing the accuracy and reliability of the tests.

Figure A1d) and e) show the varied shapes, sizes, and colorations of thrombi fragments and samples, highlighting the heterogeneity of AIS thrombi. This observation aligns with other studies reporting both inter- and intra-patient variability in thrombus physical aspects [10] [27].

After cutting, the remaining parts were combined and labelled as one 'offcut sample' kept for histological analysis. Fragments that were too small to be cut for mechanical samples were individually labelled as 'extra samples' and retained for histology. The labeling coding and one example are shown in Figure A2. Additionally, for each patient a data sheet was used to keep a record on the number of fragments from each pass, the mechanical samples prepared, and the duration of testing.

Cod format: MRCwPxTySz

MRC= abbreviation of study name
w= study ID number
P= pass
x= pass number in which the fragment was retrieved
T= thrombus/fragment
y= number attributed to a fragment found in a pass Px
S= sample
z= number of sample from fragment Ty

Example mechanical sample- MRC10P1T2S3
MRC10= Study ID
P1= first pass
T2= the second thrombus fragment in pass 1
S3= the third sample cut from fragment 2

Example extra sample- MRC4P1T1
MRC4= Study ID
P1= first pass
T1= first fragment from pass 1
*no sample was cut from this fragment

Example offcut sample- MRC17P2T1E
MRC17= Study ID
P2= second pass
T1= first thrombus fragment in pass 2
E= End and rest parts

Figure A2: Samples codding and examples from each sample category.

A3. Protocol sample preparation

Materials needed:

- absorbent pad
- thin tweezer
- Petri dish
- HEPES buffer
- ruler
- labels
- plastic box
- cutting mold
- histology blades
- Eppendorf tubes 2ml
- alcohol resistant marker
- tubes rack
- data sheet

HEPES buffer solution (2L)

Materials:

- NaCl, HEPES, MiliQ water
- precision scale
- spoon
- plastic containers
- graduated cylinder (2L)
- stirrer
- stirrer magnet

Preparation:

- Weight on the precision scale 13.44 g NaCl and 4.76 g HEPES on separate plastic containers- use small spoon.
- Put the powders in a graduated cylinder.
- Place the cylinder on the stirrer plate.
- Add 1900 mL MiliQ water and a magnet.
- Start the stirrer and wait for the powder solution to completely dissolve.
- Check with the pH-meter the solution and increase or decrease the pH to 7.4.
- Add MiliQ water to the final volume of 2 L.
- Put the HEPES buffer in a bottle with a label (name of solution, pH, date, researcher initials)

Workflow:

- When notified of eligible patient, setup lab and prepare all materials
- Collect containers with thrombus material and intervention form
- Poor in a Petri dish HEPES buffer and submerge the ruler.
- From the pass container take out each thrombus fragment and place it in the petri dish; careful to not break the fragments even more.
- Arrange labels for name coding the fragment and take pictures.
- Place the cutting mold in the plastic box and poor HEPES buffer until the mold is halfway submerged.
- If the fragment is large enough to cut a sample for mechanical testing, move it carefully in the cutting mold.
- Close mold without squashing the fragment, so that is secured during cutting. Use blades to cut in a sliding motion. Try to cut as many samples as possible from each fragment.
- Check integrity of the sample (did not fracture during cutting), and ensure it has flat top and bottom.
- If sample is good, place it back in the Petri dish and take picture with the ruler and the right label for cross sectional area measurements.
- Proceed with testing protocol; test while preparing the next sample.
- Put all the offcut pieces in an Eppendorf tube with HEPES buffer and write the sample code on the tube.
- Fill more tubes for each sample that you test.
- For the thrombus fragments that are too small, place them in the Petri dish, label them, take pictures, and put them in tubes.
- Repeat steps for all the passes.
- Fill in the data sheet for each patient.

A4. Additional Results

Table A1: Detailed baseline patient data, EVT procedure variables and outcome.

Age	median, IQR	76	36-91
Women sex	n, %	17	85
NIHSS score at admission (*n=19)	median, IQR	16	7-24
Time to treatment in minutes	median, IQR	154	80-405
Duration of EVT in minutes (*n=12)	median, IQR	38	24-151
IVT administration (*n=6)	n, %	6	30
Nr. of passes	median, IQR	2	1-5
Target occlusion location			
ICA	n, %	4	20
M1	n, %	11	55
M2	n, %	5	25
First pass device			
SR	n, %	13	65
Aspiration catheter	n, %	1	5
Combined	n, %	3	15
Final TICI score			
2b	n, %	4	20
2c	n, %	4	20
3	n, %	10	50
mRS score			
0-2	n, %	9	45
>2	n, %	7	35

ICA internal carotid artery, NIHSS National Institutes of Health Stroke Scale. TICI Thrombolysis in Cerebral Infraction, mRS modified Rankin Scale.
*The parameter has only been reported for the indicated number of patients.

After processing tissue material from all the patients, a total of 108 thrombus fragments were retrieved. From these, 138 mechanical samples were prepared. Figure A3 illustrates the number of thrombus fragments and mechanical samples for each patient.

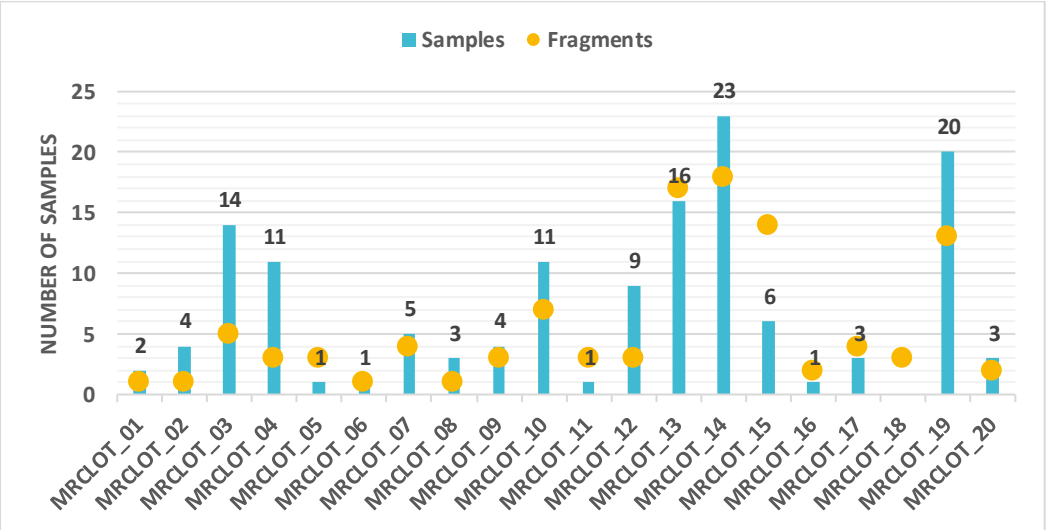

Figure A3: Number of thrombus fragments and tested samples from each patient

B

Mechanical testing

Unconfined compression testing was employed to assess the mechanical properties, particularly the viscoelastic behavior, of AIS thrombi. This testing method was selected for several reasons: in vitro thrombi are typically subjected to compressive loadings; it is a feasible testing technique given the size limitations of the retrieved thrombus compared to alternatives like tensile testing to failure; and it has been successfully used in previous studies to analyze thrombi fragments, enabling comparative results. Figure B1 illustrates the mechanical compression tester.

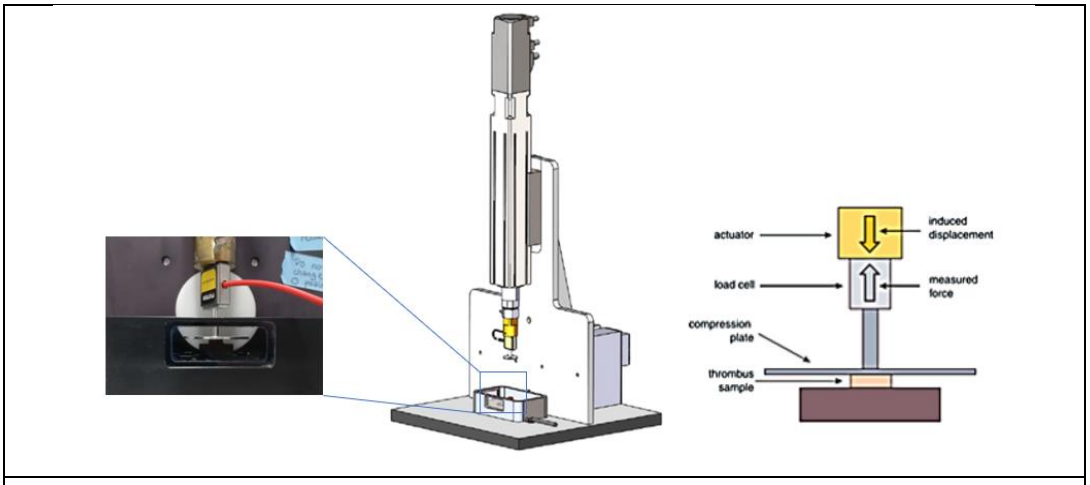

Figure B1: Mechanical compression tester. Adopted from Boodt et al. [3]

Mechanical samples were placed in the water bath of the tester filled with HEPES buffer and maintained at a constant temperature of 37°C. The samples were left to equilibrate for 5 minutes before starting the test. The compression plate was lowered 1 mm above the base of the water bath, or 2 mm for taller samples, ensuring that the plate was also submerged and in contact with the sample without exerting any pressure. This minimizes potential friction and allows radial expansion of the sample during testing.

Following the equilibration period and the stabilization of the reading signal, the test commenced. The actuator was programmed to hold for one second at the start of the test, which ensured that the reading signal was accurately processed by the software without any delay. Subsequently, the actuator compressed the sample to 80% of its original height, at a controlled strain rate of 0.1 mm/s, and then retracted at the same rate. This compression-retraction cycle was performed 20 times for each sample.

As mentioned in the scientific paper presented here, several samples were subjected to 60% compression instead of 80%. For these samples extra signal processing was done.

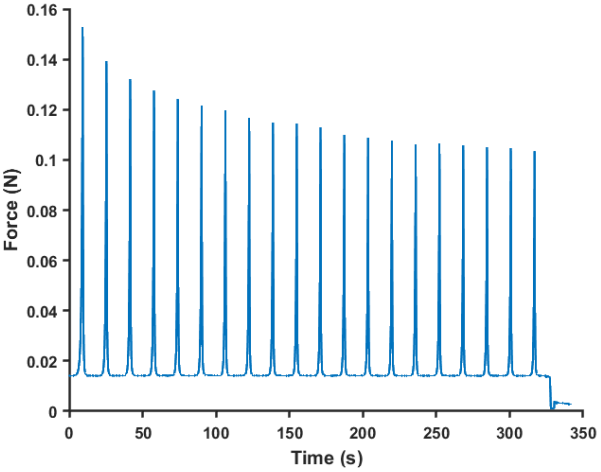

Figure B2: Force-time compression signal over 20 cycles.

B1. Signal processing

As observed in figure B2, the compression tester's output signal is in force and time. Using customized scripts in MATLAB, the data was processed to produce a typical stress-strain curve. By dividing the force by the sample's cross-sectional area, which was quantified in ImageJ as the pixel to length ratio, formula B1 was used to convert the force to nominal stress.

$$\sigma = \frac{F}{A} \tag{B1}$$

The displacement over time was determined as the product of the speed and the amount of time that had passed since the beginning of each compression cycle, considering that the sample's initial length (l_0) was 1 mm, and that displacement was applied at a constant speed of 0.1 mm/s.

$$\varepsilon = \frac{\Delta l}{l_0} \tag{B2}$$

To evaluate the stiffness, the stress- stain curve of the first loading cycle was isolated, and a linear fit was applied to the first 10% and the last 5% strain, as shown in image B3. These segments were chosen to capture the initial linear behavior and the subsequent linear response after the non-linear stiffening period.

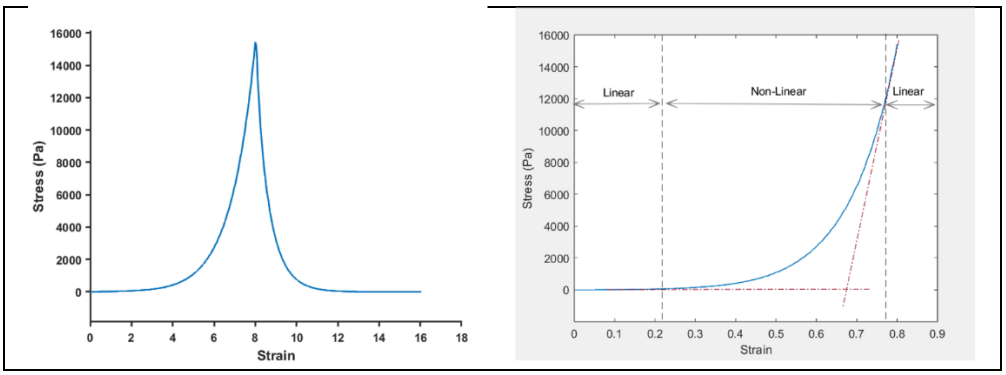

Figure B3: Example of one compression cycle, and a loading stress-strain curve.

The sample subjected to only 60% compression had the initial force-time signal shorter, meaning that each loading and unloading cycle had 12s instead of 16s. The stress-strain curve was also shorter. To use the data from these samples a Gaussian Process Regression was used to extrapolate the stress-strain curves up to 80% strain. The 'fitrgp' function in MATLAB allows for such extrapolation by defining the form of the

regression line, the type of covariance between strain pairs of points (squared exponential Kernel), the fit method of the strain points, and how the predictions of stress points to the new strain values are made.

The Kernel function used by MATALB is:

$$k(x_i, x_j) = \sigma_f^2 \exp\left(-\frac{(x_i - x_j)^2}{2l^2}\right) \quad \text{(B3)}$$

where **k** is the covariance between two strain points ($\mathbf{X_i}$ and $\mathbf{X_j}$), **σ** is the variance of the signal, and **l** is the length scale. The means of the new extrapolated strain values are obtained by using the formula:

$$\mu^* = K_*^T (K + \sigma_n^2 I)^{-1} y \quad \text{(B4)}$$

where $\mathbf{K_*}$ is the covariance matrix between the original strain values and the new extrapolated strain values, **K** is the covariance matrix of the original strain values, **σ** is the noise variance, **I** is the identity matrix, and **y** is the original stress values. The prediction for the new stress values follows a similar formula where $\mathbf{K_{**}}$ is the covariance matrix of the extrapolated strain values:

$$\Sigma^* = K_{**} - K_*^T (K + \sigma_n^2 I)^{-1} K_* \quad \text{(B5)}$$

After that the new stress-strain is fitted in the continuation of the original stress-strain obtaining a full 80% strain curve as illustrated in Figure B4.

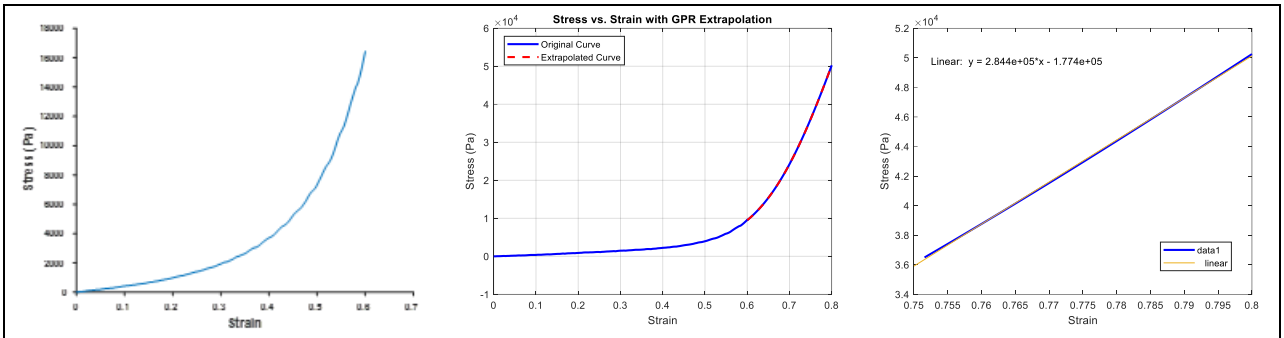

Figure B4: Stress-strain curve at 60% compression, with extrapolated signal up to 80% strain, and a linear fit at 75-80% strain for stiffness calculation.

Plotting the loading and unloading curves for each cycle allows us to visualize the hysteresis and measure the area and ratio as an indicative for the energy dissipation that takes place during deformation. The hysteresis area is defined as the area enclosed by the loading and unloading curves, while the hysteresis ration is defined as the ration between the hysteresis area to the total area under the loading curve. This approach highlights the viscoelastic and strain rate-dependent nature of the material across different cycles.

B2. Reasons for exclusion of data

Because of the soft nature of blood clots and the small dimensions of the samples, the force response was sometimes extremely small, or the compression tester intercepted a lot of noise. Figure B5 depicts a typical stress-strain curve, with low and high strain stiffness quantified accurately. At low strain (0-10%), the signal can contain minor noise peaks. However, by applying a smooth function, the signal can get more even.

On the other hand, samples where the initial signal was very low (<0.1N), or the stress-strain curve started at a negative value, were left out from the analysis. These samples had a significant level of noise, which made the identification of the true starting point of the curve challenging. This can also have an impact

on high strain stiffness assessments, as the data may not match the intended 80% strain level. Samples subjected to 60% compression that could not be properly by the Gaussian regression model fitted (the stress-strain curve was not following the usual non-linear pattern) were also excluded. Figure B6 is an example of a sample that was rejected due to signal mismatch.

In the end, 12 samples were excluded from the final analysis: one underwent a relaxation test instead of a cyclic compression test, three had a signal response smaller than 0.05 N, four had negative low strain stiffness, and four where the Gaussian extrapolation failed, resulting in no high stiffness results.

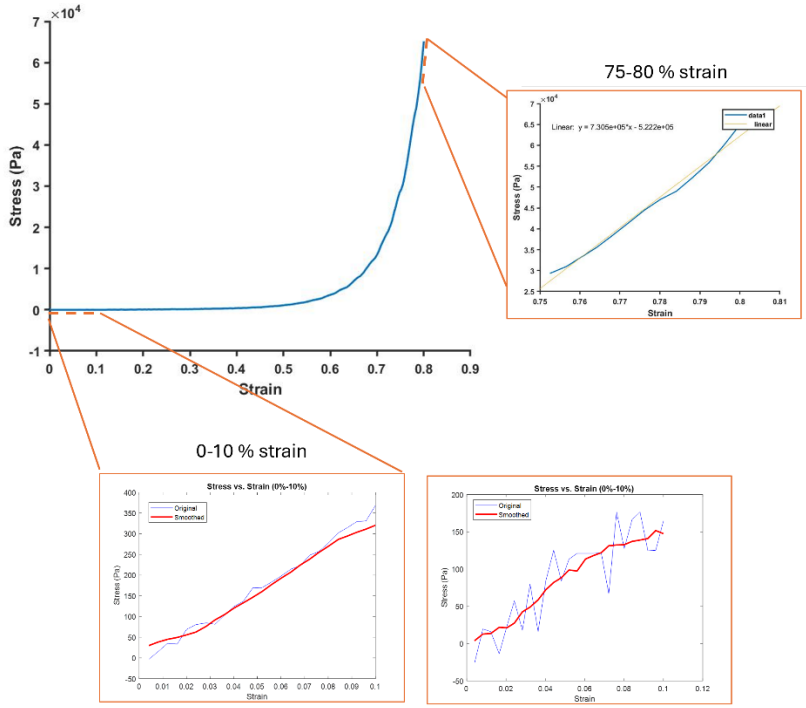

Figure B5: Normal stress strain curve and linear fit at 0-10% strain and 75-80% strain.

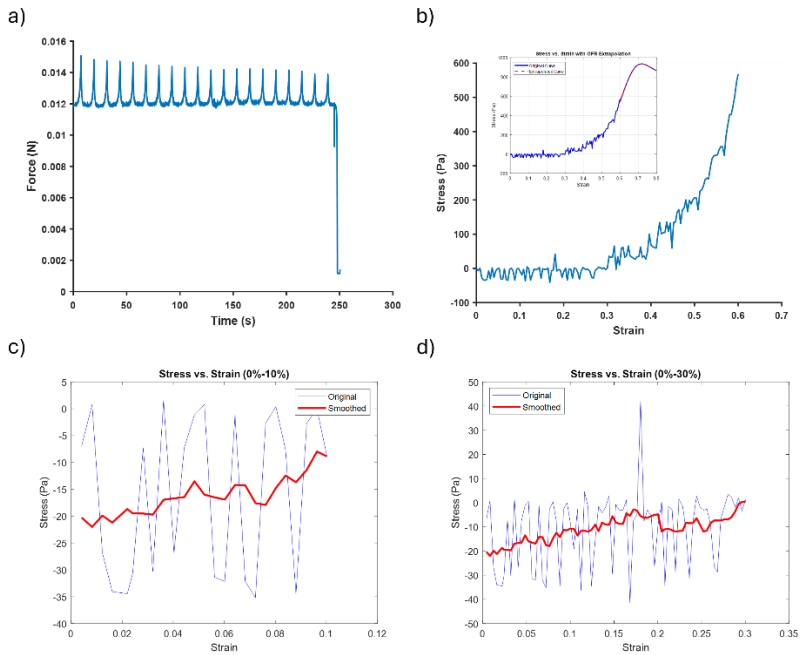

Figure B6: Mechanical sample with a) small force-time signal over the 20 cycles; b) stress-strain curve to 60% stain, and extrapolated data; c) 0-10% strain curve; d) 0-30% strain curve. Red line represents the smoothed curve.

B3. Protocol unconfined compression testing

-Place the water bath in the groove of the tester platform and couple it to the heating system and turn it on.
- Fill the water bath with HEPES buffer all the way up.
- Start the MEX2 software file and check the setting parameters: starting height, displacement, speed, number of cycles. Write the file to the hardware.
- Open LabView file and run it; the signal read by the load cell will appear.
- Tare load cell by holding the button for one second.
- Create a txt. file with the sample code and set the path of the file in LabView.
- Once the water bath is heated up, use a brush to eliminate the air bubbles from the HEPES.
- Place the sample on the stage inside the water bath and set the timer for 5 minutes.
- Lower the plate to 'starting height' and check that is touching the sample without putting any pressure- the load cell reading will have a sudden spike in the signal when the plate touches the water, followed by a … period in the signal until is stabilizing
- Start the test and check that 20 cycles run; it should take approximately 6 minutes.
- Stop recording when the test is done, and the compression plate is rising.
- Check the data in the sample file.
- Fill in the data sheet with the timing of the test.
- Move to the next sample repeating the steps form creating the file on.
- When done with all samples, close everything, and clean the tensile tester, check lab requirements for cleaning.

B4. Results

Table B1. Per patient mechanical properties of thrombi.

Patient ID	Low strain stiffness (kPa)	High strain stiffness (kPa)	Hysteresis Area (kPa)	Hysteresis Ratio (%)
MRCLOT_01	0.59	786.00	0.99	32.82
MRCLOT_02	0.59	694.33	1.18	36.20
MRCLOT_03	2.89	1131.51	2.91	32.50
MRCLOT_04	5.50	1223.21	4.57	29.69
MRCLOT_05	1.08	393.60	0.73	57.60
MRCLOT_06	2.03	1457.00	3.19	37.90
MRCLOT_07	2.68	914.12	2.70	35.72
MRCLOT_08	44.34	1120.00	12.40	35.86
MRCLOT_09	2.11	735.08	2.18	47.38
MRCLOT_10	1.34	547.10	1.19	35.57
MRCLOT_11	1.71	694.50	1.31	30.79
MRCLOT_12	0.92	487.33	0.73	38.53
MRCLOT_13	1.77	516.64	1.27	35.79
MRCLOT_14	2.55	274.06	0.54	32.69
MRCLOT_15	0.47	107.50	0.18	43.69
MRCLOT_16	3.51	284.40	0.26	36.95
MRCLOT_17	2.65	341.25	0.42	33.33
MRCLOT_19	3.33	557.78	0.60	45.84
MRCLOT_20	2.48	307.37	0.44	40.69

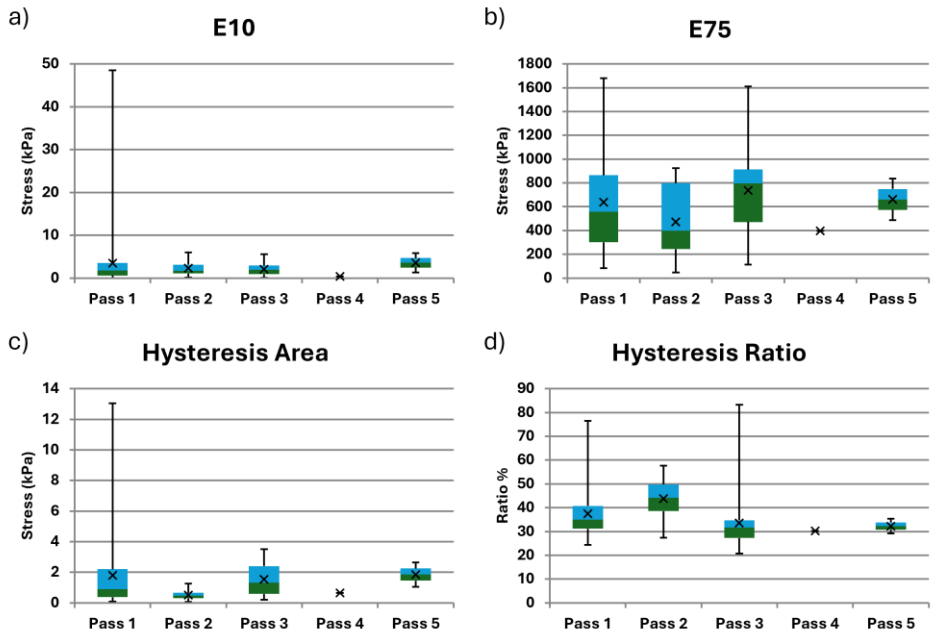

Figure B7: Per pass a) low strain stiffness; b) high strain stiffness; c) hysteresis area; d) hysteresis ratio.

C

Histology

C1. Methods

Fixation

After mechanical testing, all thrombus fragments were prepared for histology. The samples were immersed in formaldehyde (3.8-4.2% HCOH) for 24-48 hours to fixate the tissue, preserving it from autolysis and preventing further morphological changes. Following fixation, the samples were transferred back into HEPES buffer and stored at 4-8°C for no longer than two weeks. Once a batch of samples had been stored, they were prepared for the Histokinette.

Dehydration

Histology cassettes were individually prepared for each sample, with foam padding to safeguard the tissue. Gradual dehydration of the samples was carried out using Histokinette program 3, involving 12 steps transitioning from lower to higher ethanol concentrations (7 steps), succeeded by immersion in xylene (3 steps) to remove residual alcohol, and culminating in immersion in paraffin wax (2 steps).

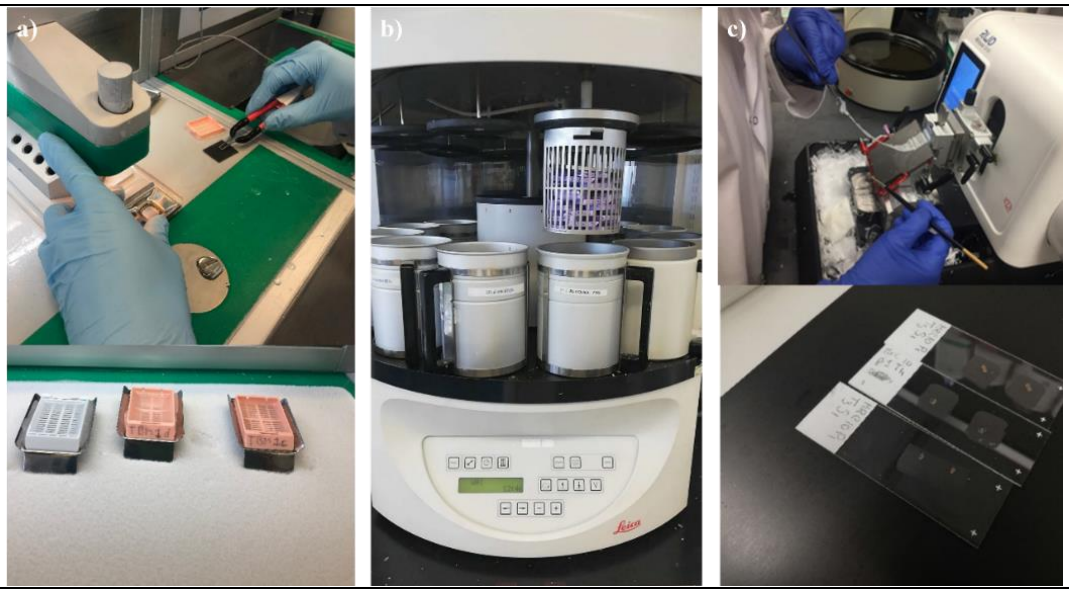

Figure C1: a) Embedding tissue samples in paraffin blocks; b) Samples put in the Histokinette for dehydration; c) Paraffin block sectioning at the Microtome and sample slides with tissue sections.

Embedding

The cassettes were removed from the Histokinette and transferred to the heated chamber of the embedder (…°). Subsequently, the tissue was carefully extracted from the cassette, and the foam padding along with the cassette lid discarded. Thrombus fragments were then positioned in cassette molds with the flat surface facing downwards, ensuring complete cross-sectional coverage during Microtome sectioning. The

molds were then filled with paraffin wax and allowed to cool on a -50°C plate.

Sectioning

The paraffin blocks were cut using a Microtome. At least 6 concomitant sections of 5 µm thickness were cut. Where possible 10 sections were cut to obtain 5 slide blades with 2 sections each. The glass slides were incubated for 24h at 40°C to dry out. The three most representative slides were used for staining.

Staining

Hematoxylin and Eosin (HE) staining stands as the foremost choice for histological tissue identification. In AIS thrombi, HE facilitates the visualization of individual components: red blood cells (RBC) appear in red, white blood cells (WBCs) in light purple, and fibrin and platelets in pink. Conversely, Masson's trichrome (MSB) staining selectively highlights RBC in yellow using Martius yellow solution, while fibrin is stained red with crystal scarlet solution, and WBCs are depicted in dark purple. Collagen and other connective tissue elements may exhibit a blue hue due to the use of methyl blue solution. Immunohistochemical CD42b staining aids in platelet identification, appearing in brown, while WBCs are represented in purple. The remaining tissue components, including RBC and fibrin, are depicted in white-gray. Figure 3 provides an illustrative example of a sample stained using all three staining techniques.

Scanning

The slides were scanned using a Nanozoomer, employing a magnification of 40x with a resolution of 0.23 µm/pixel to produce high-quality digital images. To ensure efficiency, the scanning process was conducted in batches, allowing for optimal use of time and resources. Subsequently, these digitized images were securely stored as raw .ndpi files within the research department's internal database.

Image analysis

For the quantification of sample composition, the Orbit Image Analysis (Orbit, Idorsia Ltd.; www.Orbit.bio) [8] was used. This is a machine learning software that uses selective color-based segmentation and classification to calculate percentage from the total thrombus section area. The quantification process involves custom exclusion and inclusion models trained to recognize specific cells or tissue.

Each stain requires the creation of new models to accurately quantify components. Exclusion models eliminate background and unwanted particles, retaining only the tissue area. The inclusion models are tailored to identify different cell groups, enabling the software to identify the relevant components in future images. The number of models required varies based on the color intensity of each staining. Even slides stained in the same batch may necessitate additional models for accurate quantification.

Once trained on a minimum of three images, a model can quantify tissue in other images with similar colour intensities. For this study, H&E staining samples required three exclusion and ten inclusion models due to their high staining intensity, which challenged the software's ability to discriminate between cell types. Due to the H&E lack of specificity, MSB was chosen as the primary staining method, with HE results used only for verification of the MSB results.

For the MSB stained slides images, four exclusion and three inclusion models were made. The distinct colors of the cell types are easy to distinguish and allow for efficient quantification of RBC, fibrin with platelets, and WBCs. The CD42b staining was used for platelet quantification, requiring three exclusion and one inclusion mode. An experienced pathologist, blinded to the interventional and clinical information of patients, checked the Orbit models. This rigorous validation process ensured the accuracy and reliability of the quantification results.

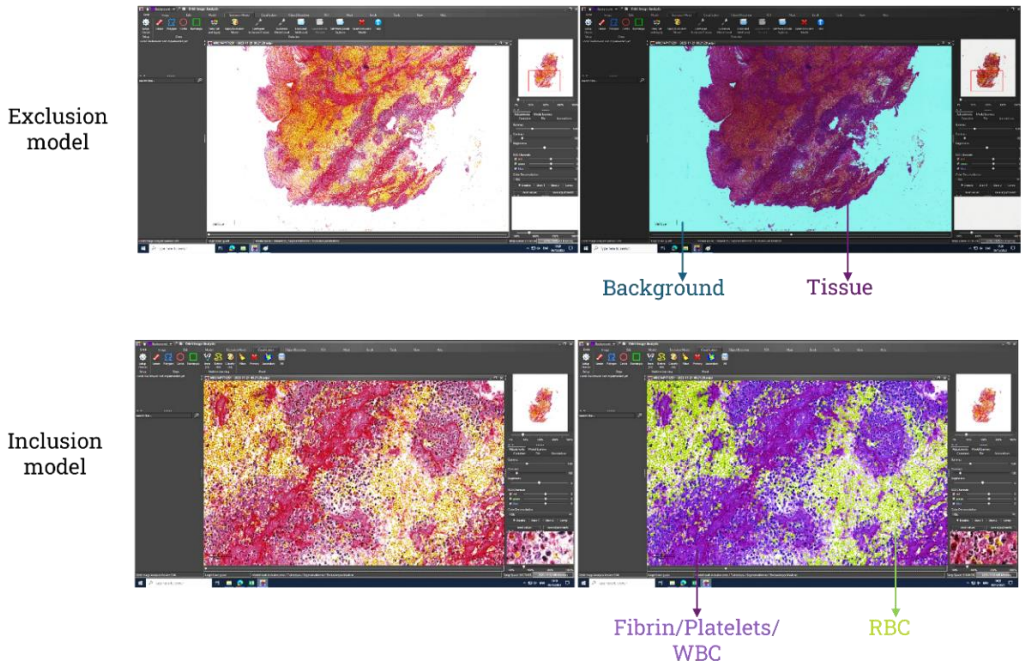

Figure C2: Exclusion and inclusion example models for MSB staining slide images.

C2. Protocol Histology sample

Materials needed:

- Eppendorf tubes 2ml
- Accu-jet pipet controller
- Serological pipette 10 ml
- Rack to hold the tubes
- Alcohol resistant marker to label the tubes
- HEPES buffer
- Formaldehyde 3.7-4.2%
- flat tweezer
- histology cassette
-Ethanol 70%, 80%, 96%, 100%
- Xylene
- Paraffin was platelets
- Embedding mold plates
- Spatula and tweezers for paraffin
- Needle for sectioning
- Brush
- Microscope slide blades
- Histology tissue blades
- Isopropanol
- microfiber cloth

1. Sample fixation

- Write with marker the sample label on the tubes X2 batches.
- Fill the first batch of tubes with HEPESS buffer.
- After each test transfer sample in tube with HEPES -use tweezer gently.
- In the fume hood fill the second batch of tubes with formaldehyde.
- When finished testing all samples transfer the tissue samples from the HEPES tubes to the formaldehyde tubes in the fume hood.

- Let the samples fixate for 24-48h
- Transfer the samples from formaldehyde to HEPES buffer and store tubes in the fridge at 4-8°C. Do not store for longer than 2 weeks.

2. Sample dehydration

- Schedule Histokinette slot time
- Label cassette and put foam pads on the bottom and on the lid of the cassette.
- Use tweezers to transfer tissue from HEPES to the cassettes, place flat surface of the sample face down, close lid carefully.
- Check containers inside Histokinette- solutions should be clean and the level high enough in the containers; If necessary, change solutions in the fume hood; Discard old solution in appropriate disposal bin.
- Put the cassette in the Histokinette' cage and set for Program 3- runs for 25 h.

3. Embedding

- Start embedding machine 1.5 h before the end time of the Histokinette to warm up the paraffin. Also, start the cooling plate.
- Take out the samples from Histokinette and put cassettes in the heating chamber of the embedder.
- Take one cassette at a time, open it carefully, detach the lid and throw it away.
- Remove top foam pad and throw away – check to not have tissue pieces stuck in the foam.
- Fill a mold plate with a bit of paraffin.
- Transfer samples in the mold, place flat side down.
- Cool down the mold for a few seconds to fixate the tissue at the bottom of the mold.
- Throw away the second foam pad and place the cassette on top of the mold plate.
- Fill the mold with paraffin till above the cassette.
- Place mold on the cooling plate.
- Take paraffin block out of the mold when cooled down.
- Clean the edges with the spatula.
- Repeat the steps for all samples.
- Stop Embedder and cooling plate when done.
- Clean molds, tweezers, spatula, and embedder machine with … to remove the paraffin wax.

4. Sectioning

- Turn on the Microtome, cooling plate, and heating plate.
- Fill the Floatation bath with …. and turn it on.
- Place the paraffin blocks on the cooling plate.
- Place a new blade on the cutting plate.
- Fix a paraffin block in the Microtome's clamps- adjust the position of the block so that is parallel to the cutting blade.
- Set the cutting at 5 µm dept.
- Start cutting- use needle to form ribbon and the brush to clean the cutting plate if to much paraffin gets stuck on it.
- Cut till you have a full cross section area of the tissue. Try to form a ribbon with at least 6 consecutive sections.
- Place ribbon in the flotation bath, use the needle or a tweezer to carefully pick up the ribbon from the cutting plate.
- Label slide blades and heat them up for a minute or two.
- Carefully break with a tweezer the ribbon into two sections each.
- Emerge one slide under the surface of the water bath and under two tissue sections, incline the slide at a 30-45° angle and capture the sections while getting the slide out of the water.
- Place slides on the heating plate till all the water drops are gone
- Repeat steps till you make 3-5 slides with two sections each for all the sample blocks.
- Place slides on a rack without touching each other and put them in the incubator for 24h to dry.

5. Staining

- Schedule staining sessions in the Histology lab.
- Follow the in-house protocols for HE, MSB, and Immunochemical CD42b staining provided by the lab technician.

6. Scanning

- Schedule Nanozoomer time slot.
- Clean slides with microfiber cloth and isopropanol.
- Prepare batches of at least 50 slides.
- Make a list with the sample's label and imported in the Nanozoomer system.
- Follow Nanozoomer training provided by the Pathology departments at Erasmus MC.
- Transfer .ndpi files to the research database.

7. Image analysis

- Follow the Orbit protocol provided by Fitzgerald et al. [8] and build inclusion and exclusion models to quantify the thrombus components.
- Run the models for all pictures and collect results in a database table.

C3. Results

Structural aspects

Figure C3 shows 5 samples with low to high concentration of RBC. All samples exhibit complex structures with both dense areas, where RBC are compacted together within fibrin rich areas, and less dense areas where thinner fibrin strands are dispersed randomly, and the RBC are less packed together. Samples with higher concentrations of fibrin show that fibrin bundles follow different patterns which can reflect the thrombus formation process in vivo. Samples with very dense structures had often older compacted RBC and polyhedrocytes RBC, which make the thrombus less permeable and therefore more resistant to retrieval [22]. Furthermore, thrombi with high content of polyhedrocytes RBC are correlated with worse functional outcomes after EVT [22].

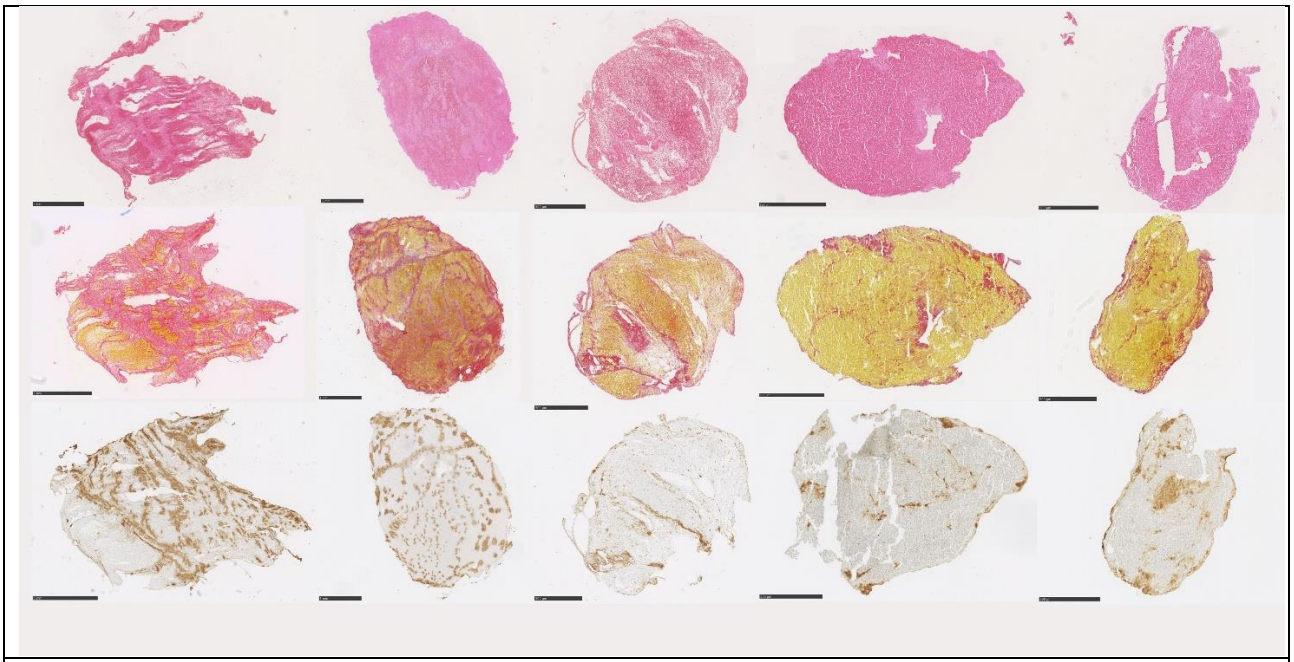

Figure C3: Mechanical samples arranged by varying percentages of RBC, increasing from left to right. Each sample is stained with HE, MSB, and CD42B, displayed from top to bottom. Scale bars represent 1 mm and 500 µm.

MSB vs. H&E

The comparison between MSB and H&E was done to check the agreement between the two staining. The fibrin/platelets and RBC quantifications from the tissue slides were plotted and a linear regression model was applied (Figure 5, Scientific paper). To check if the model was adequately capturing the relation between MSB and H&E measurements for both thrombus components, a residual analysis was performed. Figure C4 shows the graphical results from the residual analysis. Residuals versus fitted values (here MSB measurements) reveal if the linearity assumption is violated or not based on the presence of data patterns. In this case no clear patterns were observed, as data points were both spread out and clustered. The variance of the residuals was relatively constant and no funnel shape pattern that could indicate heteroscedasticity was shown. The histogram shows that the residuals were independent from each other and followed an approximately normal distribution. This was also seen in the quantile-quantile plot where a few deviations at the tails were presented but the overall data points were following the normal distribution line.

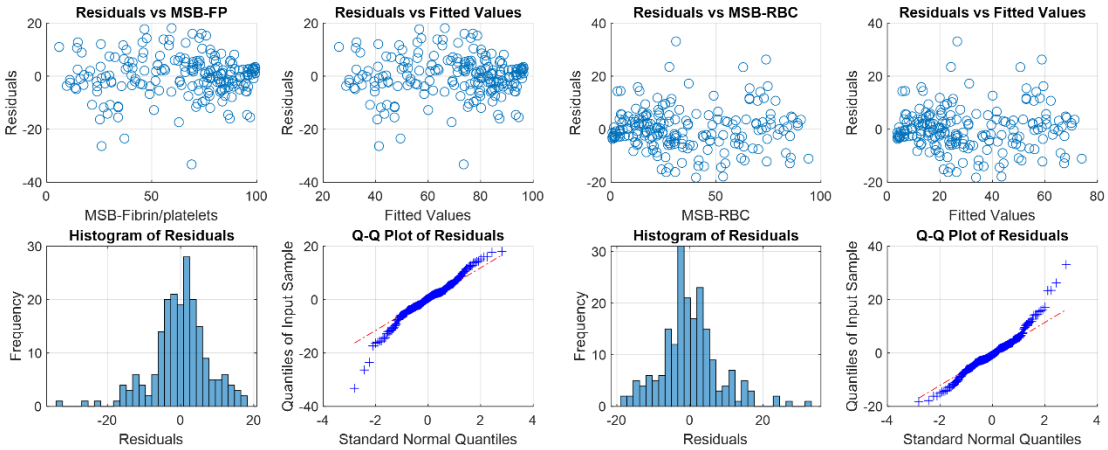

Figure C4: Residual analysis graphs for fibrin platelets (left), and RBC (right).

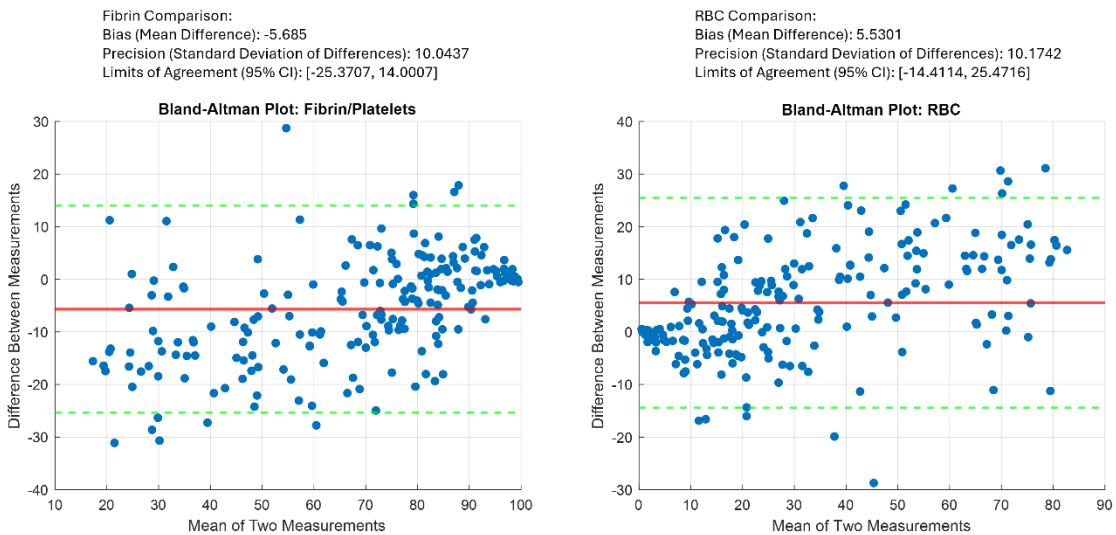

Figure C5: Bland Alman analysis for fibrin/platelets and RBC from MSB and H&E. Red line indicates mean difference. Green dotted line represents limits of agreement (mean of the differences ± 1.96 x SD of the differences).

Bland Alman analysis

A Bland Alman test was preformed to further investigate the agreement between MSB and H&E (Figure C5). The data points representative of the difference between the measurements on the two stainings follow a funnel shape pattern that in this case means the consistency across measurements was not uniform. The mean difference between the two methods across all measurements was close to zero indicating minimal systematic bias between the MSB and H&E quantification for both fibrin/platelets and RBC. On the fibrin/platelets graph the mean difference was lower than 0, which means that the MSB measurements of fibrin/platelets were lower than the ones on H&E. The reverse can be said for RBC.

The wide range of limits of agreement are another indicative of inconsistent agreement across measurements, between MSB and HE methods. This shows that there were samples where the composition was overestimated or underestimated on the H&E compared with MSB. Some differences pass the limits of agreement, which could be attributed to outliers or samples where the tissue slides from H&E were having similar pink and red hues for different components making the quantification less accurate.

Considering all this H&E was only employed in this study as a validation step for the RBC and fibrin/platelets quantification from the MSB slides; the final analysis and correlation associations with mechanical properties were based solely on the results from MSB and CD42b stainings.

Thrombus composition per patient

Table C1 shows the quantification results for fibrin/platelets, RBC, and platelets. The average percentage per patient was calculated by using only the samples with complete quantifications from all 3 stainings.

Table C1: Histological composition results per patient. All numbers represent percentage in relation to the total tissue area.

Study ID	MSB		H&E		CD42b
	Fibrin/platelets	RBC	Fibrin/platelets	RBC	Platelets
MRCLOT_1	67.29	32.70	75.95	23.94	25.86
MRCLOT_2	49.02	50.97	64.36	35.63	34.76
MRCLOT_3	80.44	19.55	82.54	17.45	53.28
MRCLOT_4	80.81	19.18	80.25	19.74	46.45
MRCLOT_5	72.23	27.76	71.65	28.34	51.35
MRCLOT_6	89.42	10.58	86.69	13.31	66.30
MRCLOT_7	73.16	26.83	71.70	28.29	52.62
MRCLOT_8	98.80	1.19	97.87	2.12	27.42
MRCLOT_9	98.26	1.73	98.12	1.87	77.47
MRCLOT_10	31.38	68.47	42.27	57.72	20.64
MRCLOT_11	57.58	42.42	62.90	37.09	41.04
MRCLOT_12	21.60	78.39	37.00	62.99	25.27
MRCLOT_13	62.24	36.79	69.14	30.85	35.80
MRCLOT_14	82.97	17.02	88.42	11.55	73.59
MRCLOT_15	58.49	41.50	71.72	28.25	33.11
MRCLOT_16	94.56	5.43	83.62	16.38	46.66
MRCLOT_17	83.48	16.51	83.95	16.04	36.10
MRCLOT_18	89.87	10.12	90.09	9.90	28.21
MRCLOT_19	58.57	41.42	65.16	34.83	39.47
MRCLOT_20	49.85	50.14	39.56	60.43	50.40

D

Mechanical properties and composition

Linear regression

To determine the relation between mechanical properties and compositional elements, linear regression models were used. For high strain stiffness in relation to fibrin/platelets and RBC a simple linear model was fitted to the entire range of the data, while for any other relationships a linear piecewise model was used to determine the different inflection points where the variables are changing trends. These points were chosen based on the visual inspection of the data between two variables. A Chow test was conducted to confirm if the breakpoints represented a structural break in the data. The hypothesis was that the coefficients of the two regression segments do not significantly differ from one another. By using formula D1, F statistic was calculated and compared with F critic.

$$F = \frac{(s_c - (s_1 + s_2))/k}{(s, + s_2)/(n_1 + n_2 - 2k)} \quad \text{(D1)}$$

where $\mathbf{S_c}$ is the sum of squared residuals for the entire data, $\mathbf{S_1}$ and $\mathbf{S_2}$ are the sum of squared residual for every data segment, $\mathbf{n_1}$ and $\mathbf{n_2}$ are the sample sizes for each segment, and **k** is the total number of parameters in the model. If the F statistic was greater than the F critic the null hypothesis was rejected, indicating a significant breakpoint in the data.

Residual analysis

A residual analysis was carried out for each linear regression model that connected a mechanical variable to a thrombus component. The residuals results are shown in Figures D1, D2, and D3. Given the large number of correlations found here, a broad interpretation is provided.

All regression models showed residuals that were uniformly distributed around zero, without any apparent patterns that would have suggested significant deviations from linearity. The residuals seemed to capture adequately the relationship between the two variables in the regression models. A few deviations and outliers were present at the quantile tails of the residual distribution, which otherwise followed a roughly normal distribution.

In summary, all the linear models appear to suit the various relationships between composition and mechanical properties fairly well. However, the small deviations from the residuals indicate that more robust models should be used to capture the complex interplay between mechanics and composition.

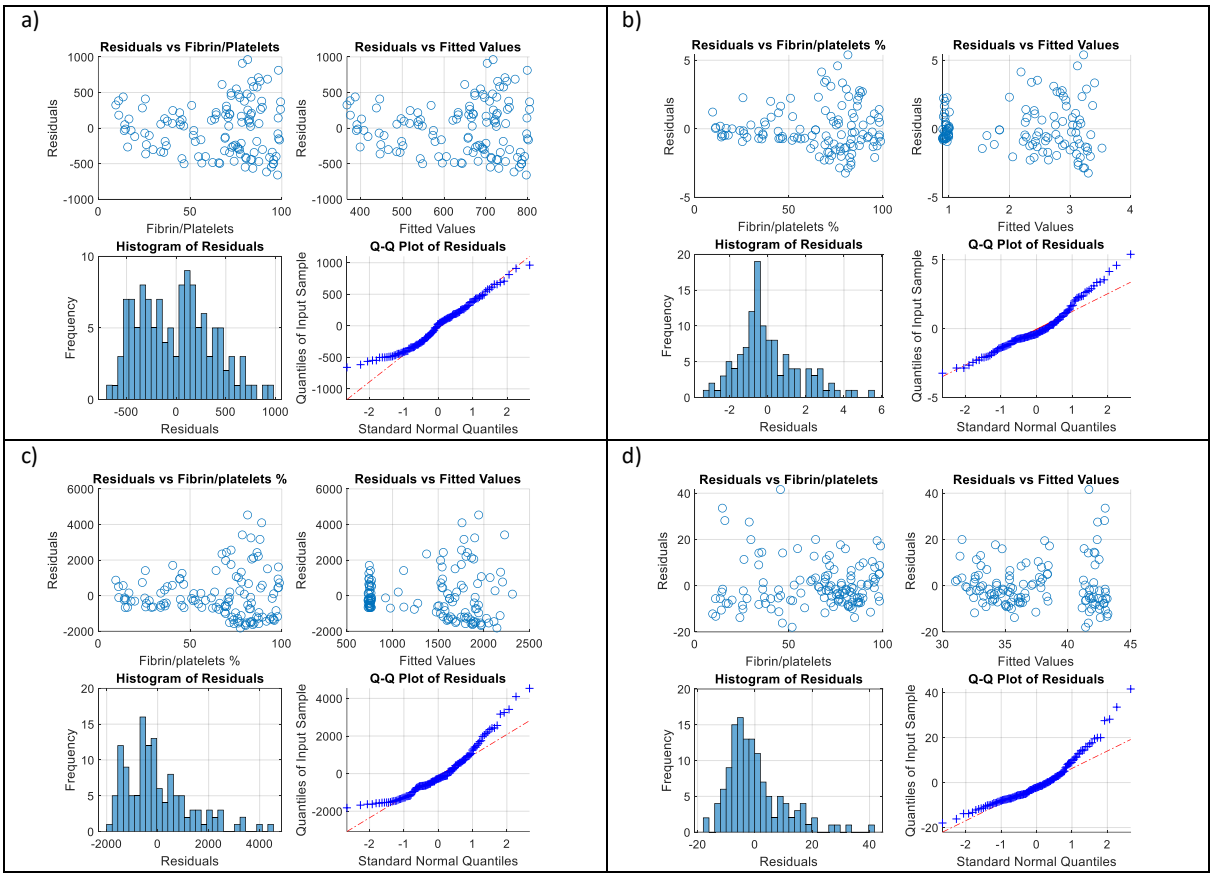

Figure D1: Residual analysis for linear regression models between fibrin/platelets and high strain stiffness (a), low strain stiffness (b), hysteresis area (c), hysteresis ratio (d).

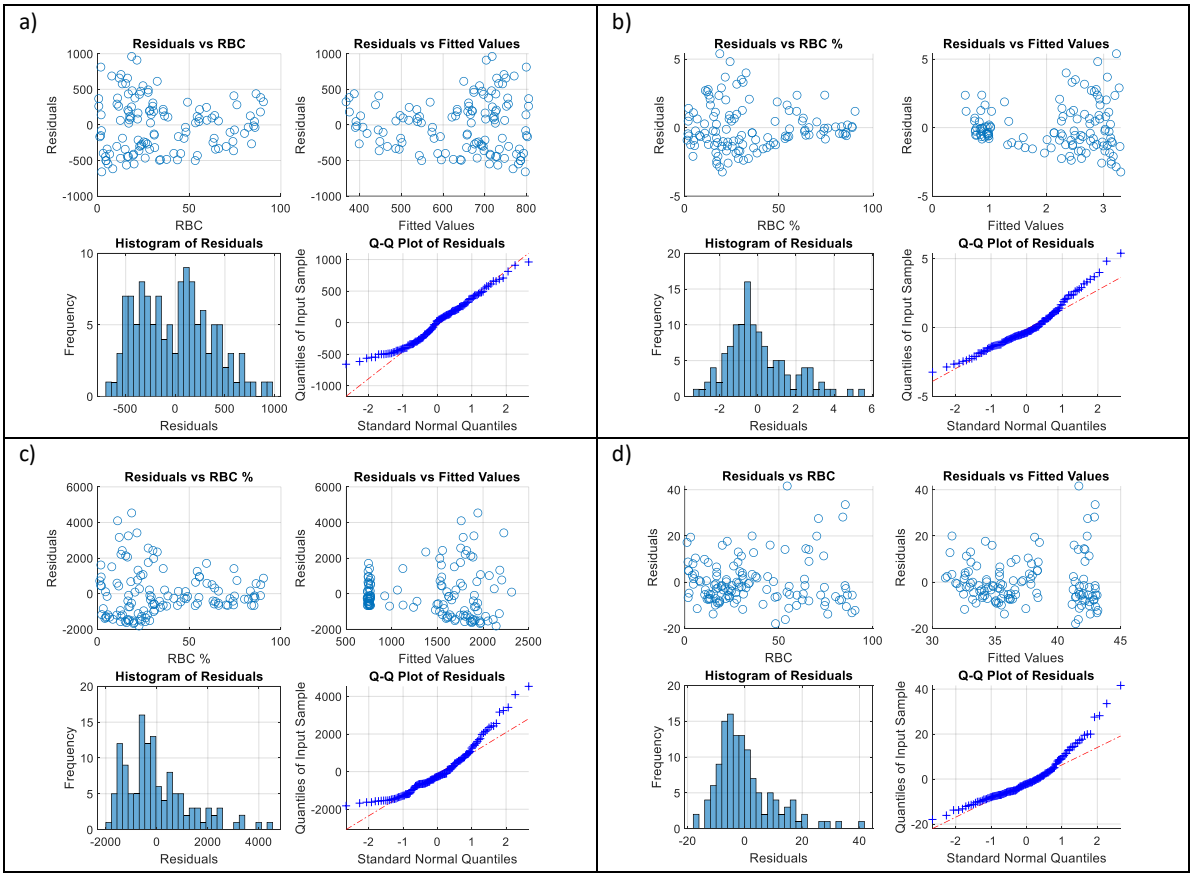

Figure D2: Residual analysis for linear regression models between RBC and high strain stiffness (a), low strain stiffness (b), hysteresis area (c), hysteresis ratio (d).

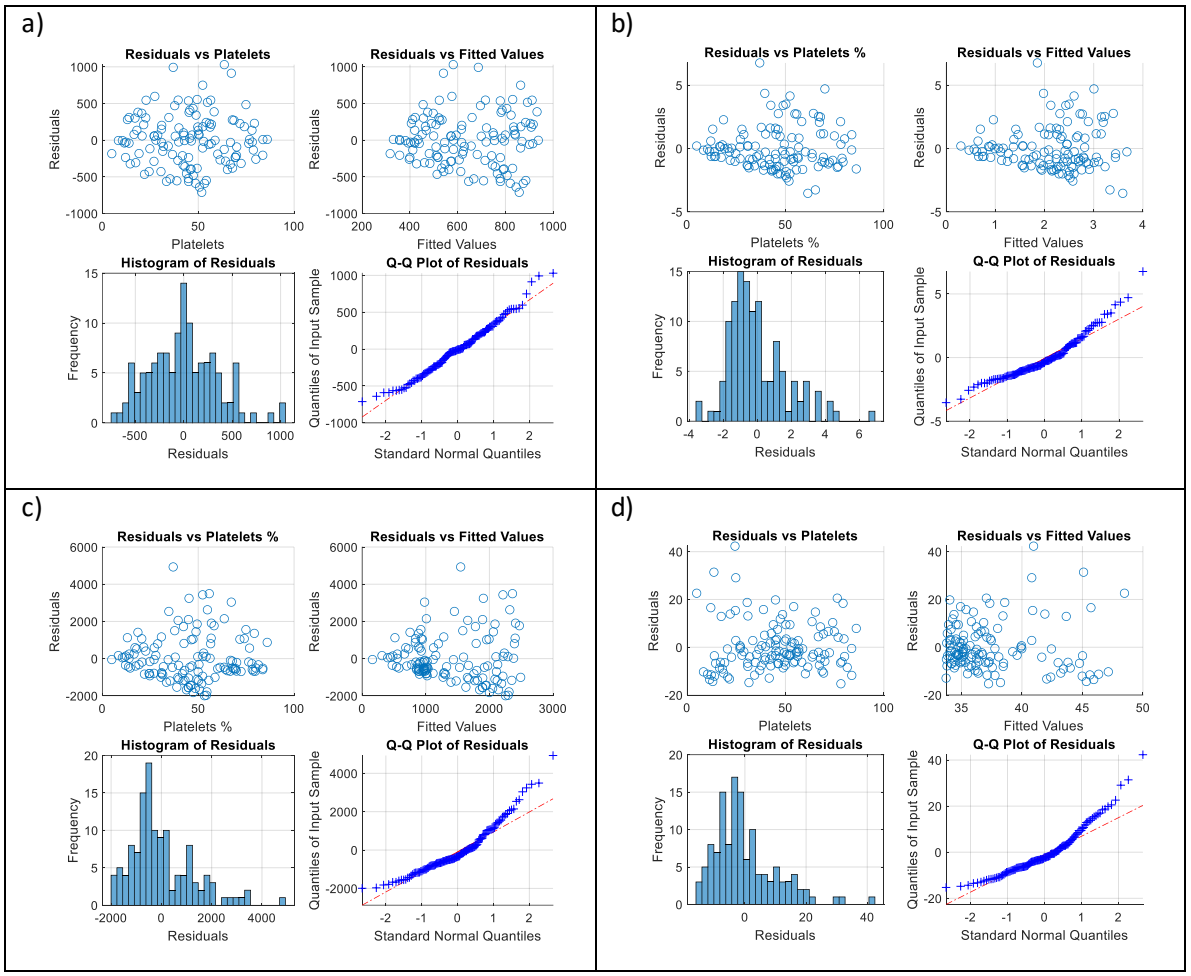

Figure D1: Residual analysis for linear regression models between platelets and high strain stiffness (a), low strain stiffness (b), hysteresis area (c), hysteresis ratio (d).

F

MATLAB SCRIPTS

Calculation of mechanical properties

Table F1: MATLAB Code to calculate low-strain stiffness and high-strain stiffness.

```
clc;
clear;
close all;
% Specify the folder to save the figures
saveFolder = 'D:\Master Delft\Thesis project\Thesis mechanics\MRCLOT_16\Mechanical files';
% Path to the data file
dataFile = 'MRCLOT_16_P1_T2_S1.txt';
% Read the data from the text file
opts = detectImportOptions(dataFile);
opts = setvartype(opts, {'Var1'}, 'datetime');
opts = setvaropts(opts, 'Var1', 'InputFormat', 'dd/MM/yyyy HH:mm:ss.SSS');
T = readtable(dataFile, opts);
% Extract columns
timestamp = T.Var1;
force = T.Var2;
% Convert timestamps to time in seconds since the first timestamp
timeSec = seconds(timestamp - timestamp(1));
time = round(timeSec, 3); % Round to three decimal places
% Plot the force versus time
PlotFigures(time,force,'Time (s)','Force (N)',saveFolder)
%% Crop data 20 loops
% Define the start and end times of the desired data range
startTime = 1.115; % Given as start of first cycle
endTime = 244.996;  % Given as end of last cycle in the dataset

% Find the indexes for the start and end times
startIdx = find(time >= startTime, 1, 'first'); % Finds the index of the first occurrence greater than or equal to
startTime
endIdx = find(time <= endTime, 1, 'last'); % Finds the index of the last occurrence less than or equal to
endTime

% Crop and zero the data
newtime = time(startIdx:endIdx) - time(startIdx); % Zero the time at the start of the cropping interval
newforce = force(startIdx:endIdx) - force(startIdx); % Extract the force data for the cropped time interval (no
zeroing unless needed)

% Constants and Initial conditions
originalLength_mm = 1; % original length in mm
displacement_mm = 0.1; % displacement in mm
CSA = 0.000002836  ; % Cross-sectional area in square meters

% Calculate strain and stress
Strain = displacement_mm / originalLength_mm;
Stress = newforce ./ CSA; % Calculate stress in Pascals
%Stress_kPa = Stress_Pa / 1000; % Convert stress to kilopascals
```

```
% Plotting stress vs. time using a custom plotting function
PlotFigures(newtime, Stress, 'Strain', 'Stress (Pa)', saveFolder);
%% Write 20 loops stress-time data to an Excel file
WriteToExcel('Time',  newtime ,'A','00_20cycles_data_new.xlsx');
WriteToExcel('Stress (Pa)', Stress ,'B','00_20cycles_data_new.xlsx');
%% Loading part only Dynamic Peak Analysis Configuration
desiredCycleNumber = input('Enter the cycle number to analyze (1-20): ');

% Find all peaks
[peakValues, indexes] = findpeaks(force, 'MinPeakHeight', 0.02);

% Check if there are enough peaks
if length(indexes) < desiredCycleNumber
    error('Not enough peaks detected to analyze the desired cycle number.');
end

% Select the specific peak for the desired cycle
peakIndex = indexes(desiredCycleNumber);
peakTime = time(peakIndex);
%peakTime = 9.121 ;

% Define start and end times relative to the selected peak
startLoadingTime = peakTime - 6;  % 8 seconds before the peak for loading
endUnloadingTime = peakTime;

[~, startIdx] = min(abs(time - startLoadingTime));
[~, endIdx] = min(abs(time - endUnloadingTime));

% Extracting displacement and force data for the loading part
newTime = time(startIdx:endIdx) - time(startIdx);
newForce = force(startIdx:endIdx) - force(startIdx);
displacement = newTime * 0.1; % Assuming a displacement rate of 0.1 mm/s

% Plotting displacement vs. force
PlotFigures(-displacement, -newForce, 'Displacement (mm)', 'Force (N)', saveFolder);

% Calculating strain and stress
area = 0.000002836  ; % CSA in m2
Strain = displacement / 1; % Assuming a gauge length of 1 mm or 2mm in rare cases
Stress = newForce / area;

% Plotting strain vs. stress
PlotFigures(Strain, Stress, 'Strain', 'Stress (Pa)', saveFolder);
%% First loading part write to excel
WriteToExcel('Strain',  Strain ,'A','01_First_loading_part_new.xlsx');
WriteToExcel('Stress (Pa)', Stress ,'B','01_First_loading_part_new.xlsx');
%% Extrapolation 75%-80%
close all

% Extrapolate the stress-strain curve to reach 0.8 strain if it doesn't already
maxStrain = max(Strain);
if maxStrain < 0.8
    % Define the strain range for extrapolation
    extrapolatedStrain = linspace(maxStrain, 0.8, 100)';
    % Use spline interpolation for better fit to the existing data
    splineFit = spline(Strain, Stress);
    % Calculate the corresponding stress values using the spline fit
    extrapolatedStress = ppval(splineFit, extrapolatedStrain);
    % Append the extrapolated data to the original data
    Strain = [Strain; extrapolatedStrain];
    Stress = [Stress; extrapolatedStress];
end
% Plot the original and extrapolated stress-strain curve
figure;
```

```
plot(Strain, Stress, 'b-', 'LineWidth', 2);
hold on;
if maxStrain < 0.8
   plot(extrapolatedStrain, extrapolatedStress, 'r--', 'LineWidth', 2);
   legend('Original Curve', 'Extrapolated Curve');
else
   legend('Original Curve');
end
title('Stress vs. Strain with Extrapolation');
xlabel('Strain');
ylabel('Stress (Pa)');
%% Stiffness 75%-80%
close all

[~,newstartIdx] = min(abs(Strain-0.55));
[~,newendIdx] = min(abs(Strain-0.60));
highstrain = Strain(newstartIdx+1:newendIdx);
highstress = Stress(newstartIdx+1:newendIdx);
[ultimateStress, idxUltimate] = max(highstress);  % max function also returns the index of the max value
ultimateStrain = highstrain(idxUltimate);

% Plot the stress-strain curve for this range
figure;
plot(highstrain, highstress, 'b-', 'LineWidth', 2);
title(sprintf('Stress vs. Strain (75%%-80%%), Ultimate Stress: %.2f Pa at %.2f%% Strain', ultimateStress,
ultimateStrain*100));
xlabel('Strain');
ylabel('Stress (Pa)');

%PlotFigures(highstrain, highstress,'Strain','Stress (Pa)', saveFolder)
%% 0%-10%
close all

[~,lstartIdx] = min(abs(Strain-0));
[~,lendIdx] = min(abs(Strain-0.10));
lowstrain = Strain(lstartIdx+1:lendIdx);
lowstress = Stress(lstartIdx+1:lendIdx);

%PlotFigures(Strain, Stress,'Strain','Stress (Pa)', saveFolder)
PlotFigures(lowstrain, lowstress,'Strain','Stress (Pa)', saveFolder)
%% 0%-10%
close all

[~,lstartIdx] = min(abs(Strain-0));
[~,lendIdx] = min(abs(Strain-0.10));
lowstrain = Strain(lstartIdx+1:lendIdx);
lowstress = Stress(lstartIdx+1:lendIdx);
smoothedStress = smoothdata(lowstress, 'movmean', 10);  % Using moving average with a window of 10

% Plotting the original and smoothed stress-strain curves
figure;
%plot(lowstrain, lowstress, 'b-', 'DisplayName', 'Original'); % add if you want the original signal as well
hold on;
plot(lowstrain, smoothedStress, 'r-', 'LineWidth', 2, 'DisplayName', 'Smoothed');
title('Stress vs. Strain (0%-10%)');
xlabel('Strain');
ylabel('Stress (Pa)');
legend show;

%saveFolder = 'D:\Master Delft\Thesis project\Thesis mechanics\MRCLOT_01\Compression files'; % Define
your save folder path
%saveas(gcf, fullfile(saveFolder, 'Smoothed_Stress_Strain_0_10.png'));
```

Table F2: MATLAB Code to calculate hysteresis low-strain stiffness and high-strain stiffness.

```
%% Initialize and Load Data
clc;
clear;
close all;
% Specify the folder to save the figures
saveFolder = 'D:\Master Delft\Thesis project\Thesis mechanics\MRCLOT_16\Mechanical files';
% Path to the data file
dataFile = 'MRCLOT_16_P1_T2_S1.txt';
% Read the data from the text file
opts = detectImportOptions(dataFile);
opts = setvartype(opts, {'Var1'}, 'datetime');
opts = setvaropts(opts, 'Var1', 'InputFormat', 'dd/MM/yyyy HH:mm:ss.SSS');
T = readtable(dataFile, opts);
% Extract columns
timestamp = T.Var1;
force = T.Var2;
% Convert timestamps to time in seconds since the first timestamp
timeSec = seconds(timestamp - timestamp(1));
time = round(timeSec, 3); % Round to three decimal places
% Plot the force versus time
PlotFigures(time,force,'Time (s)','Force (N)',saveFolder)
%% Loading part only Dynamic Peak Analysis Configuration
desiredCycleNumber = input('Enter the cycle number to analyze (1-20): ');

% Find all peaks
[peakValues, indexes] = findpeaks(force, 'MinPeakHeight', 0.02);

% Check if there are enough peaks
if length(indexes) < desiredCycleNumber
   error('Not enough peaks detected to analyze the desired cycle number.');
end

% Select the specific peak for the desired cycle
peakIndex = indexes(desiredCycleNumber);
peakTime = time(peakIndex);
%peakTime = 9.121 ;

% Define start and end times relative to the selected peak
startLoadingTime = peakTime - 6;  % 8 seconds before the peak for loading
endUnloadingTime = peakTime;

[~, startIdx] = min(abs(time - startLoadingTime));
[~, endIdx] = min(abs(time - endUnloadingTime));

% Extracting displacement and force data for the loading part
newTime = time(startIdx:endIdx) - time(startIdx);
newForce = force(startIdx:endIdx) - force(startIdx);
displacement = newTime * 0.1; % Assuming a displacement rate of 0.1 mm/s

% Plotting displacement vs. force
PlotFigures(-displacement, -newForce, 'Displacement (mm)', 'Force (N)', saveFolder);

% Calculating strain and stress
area = 0.000002836  ; % CSA in m2
strain = displacement / 1; % Assuming a gauge length of 1 mm
stress = newForce / area;

% Plotting strain vs. stress
PlotFigures(strain, stress, 'Strain', 'Stress (Pa)', saveFolder);

%% Calculate the area under the loading curve
loadingArea = trapz(strain, stress);
disp(['Area under the loading curve for Cycle ', num2str(desiredCycleNumber), ': ', num2str(loadingArea), '
```

```
square units']);
xlswrite('04_loadArea.xlsx', loadingArea', '16P1T2S1',  'A20');% change sheet and line
%% Dynamic Peak Analysis Configuration
desiredCycleNumber = input('Enter the cycle number to analyze (11-20): '); % User inputs which cycle to
analyze

% Find all peaks
[peakValues, indexes] = findpeaks(force, 'MinPeakHeight', 0.02);

% Check if there are enough peaks
if length(indexes) < desiredCycleNumber
   error('Not enough peaks detected to analyze the desired cycle number.');
end

% Select the specific peak for the desired cycle
peakIndex = indexes(desiredCycleNumber);
peakTime = time(peakIndex);
%peakTime = 9.121 ;

% Define start and end times relative to the selected peak
startLoadingTime = peakTime - 6;  % 8 seconds before the peak for loading
endUnloadingTime = peakTime + 6;  % 8 seconds after the peak for unloading

[~, startIdx] = min(abs(time - startLoadingTime));
[~, endIdx] = min(abs(time - endUnloadingTime));

% Extract Force Data for Loading and Unloading
newtime = time(startIdx:endIdx) - time(startIdx);
newforce = force(startIdx:endIdx) - force(startIdx);
displacement = newtime * 0.1; % Assuming a displacement rate of 0.1 mm/s

% Calculate Strain and Stress
area = 0.000002836  ;  % Cross-sectional area in square meters
Strain = displacement / 1;  % Normalizing displacement to an arbitrary gauge length
Stress = newforce / area;  % Converting force to stress

%% Plotting
figure;
plot(Strain, Stress, 'LineWidth', 2);
xlabel('Strain');
ylabel('Stress (Pa)');
title(sprintf('Stress vs. Strain for Cycle %d', desiredCycleNumber));
grid on;
%saveas(gcf, fullfile(saveFolder, sprintf('Stress_Strain_Cycle_%d.png', desiredCycleNumber)));

%% Calculate the Total Area Under the Curve
total_area = trapz(Strain, Stress);
disp(['Total area under the curve for Cycle ', num2str(desiredCycleNumber), ': ', num2str(total_area), '
square units']);
xlswrite('05_20loopsArea.xlsx', total_area', '16P1T2S1',  'A20');% change sheet and line
%% Hystersis
close all

jieshutime = peakTime + 6;
[~,jieshuIdex]=min(abs(time-jieshutime));
jieshuTime=time(jieshuIdex);
endIdx=jieshuIdex;
newtime =time(startIdx:endIdx)-time(startIdx); %zero the time
newforce = force(startIdx:endIdx)-force(startIdx); %zero the force
Strain2=newtime.*(newtime<=(peakTime-startLoadingTime))*0.1+(0.1*(peakTime-startLoadingTime)-
0.1*(newtime-(peakTime-startLoadingTime))).*(newtime>(peakTime-startLoadingTime));
Stress2=newforce./area; %CSA in m2
%% Hystersis stress strain first loop
%WriteToExcel('Strain',  Strain2 ,'A','02_Hystersis_first_loop_new.xlsx');
%WriteToExcel('Stress (Pa)', Stress2 ,'B','02_Hystersis_first_loop_new.xlsx');
```

```
%% Hystersis stress strain all loop
WriteToExcel('Strain', Strain2 ,'A','03_Hystersis_all_loop_16P1T2S1_new.xlsx');%change sample name
WriteToExcel('stress (Pa)', Stress2 ,'B','03_Hystersis_all_loop_16P1T2S1_new.xlsx');%change sample name
%% Write to excel the hysteresis area
x=Strain2;
y=Stress2;
%area = polyarea(x,y);
hysteresisArea= trapz(x,y);% the hysteresis area the red part
disp(['hysteresisArea for Cycle', num2str(desiredCycleNumber), ': ', num2str(hysteresisArea)])
xlswrite('06_Hysteresis_Area.xlsx', hysteresisArea, 'Sheet1', 'A20');%change sheet and line
%% Hysteresis ratio
hysteresisRatio = (hysteresisArea / loadingArea) * 100;
disp(['Hysteresis ratio for Cycle ', num2str(desiredCycleNumber), ': ', num2str(hysteresisRatio), '%']);
xlswrite('07_Hysteresis_Ratios.xlsx', hysteresisRatio, 'Sheet1', 'A20');%change sheet and line
%% Plotting the Hysteresis Loop
figure;
plot(Strain2, Stress2, 'b-', 'LineWidth', 0.2);
title('Hysteresis Loop');
xlabel('Strain');
ylabel('Stress (Pa)');
%fill(x,y, [0.4660 0.6740 0.1880]);
hold on;
fill(Strain2, Stress2, [0 0.4470 0.7410], 'FaceAlpha', 0.2);
hold off;
%grid on;
```

Table F3: MATLAB Code for extrapolation of stress-strain curve

```
clc;
clear;
close all;
% Specify the folder to save the figures
saveFolder = 'D:\Master Delft\Thesis project\Thesis mechanics\MRCLOT_16\Mechanical files';
% Path to the data file
dataFile = 'MRCLOT_16_P1_T2_S1.txt';
% Read the data from the text file
opts = detectImportOptions(dataFile);
opts = setvartype(opts, {'Var1'}, 'datetime');
opts = setvaropts(opts, 'Var1', 'InputFormat', 'dd/MM/yyyy HH:mm:ss.SSS');
T = readtable(dataFile, opts);
% Extract columns
timestamp = T.Var1;
force = T.Var2;
% Convert timestamps to time in seconds since the first timestamp
timeSec = seconds(timestamp - timestamp(1));
time = round(timeSec, 3); % Round to three decimal places
% Plot the force versus time
PlotFigures(time,force,'Time (s)','Force (N)',saveFolder)
%% Dynamic Peak Analysis Configuration
desiredCycleNumber = input('Enter the cycle number to analyze (1-20): ');

% Find all peaks
[peakValues, indexes] = findpeaks(force, 'MinPeakHeight', 0.02);

% Check if there are enough peaks
if length(indexes) < desiredCycleNumber
    error('Not enough peaks detected to analyze the desired cycle number.');
end

% Select the specific peak for the desired cycle
peakIndex = indexes(desiredCycleNumber);
peakTime = time(peakIndex);

% Define start and end times relative to the selected peak
startLoadingTime = peakTime - 6;  % 6 seconds before the peak for loading
endUnloadingTime = peakTime;

[~, startIdx] = min(abs(time - startLoadingTime));
[~, endIdx] = min(abs(time - endUnloadingTime));

% Extracting displacement and force data for the loading part
newTime = time(startIdx:endIdx) - time(startIdx);
newForce = force(startIdx:endIdx) - force(startIdx);
displacement = newTime * 0.1; % Assuming a displacement rate of 0.1 mm/s

% Plotting displacement vs. force
PlotFigures(-displacement, -newForce, 'Displacement (mm)', 'Force (N)', saveFolder);

% Calculating strain and stress
area = 0.000002836;  % CSA in m2
Strain = displacement / 1; % Assuming a gauge length of 1 mm or 2mm in rare cases
Stress = newForce / area;

% Plotting strain vs. stress
PlotFigures(Strain, Stress, 'Strain', 'Stress (Pa)', saveFolder);

%% Extrapolation 75%-80%
close all

% Define the strain range for extrapolation
extrapolatedStrain = linspace(max(Strain), 0.8, 100)';
```

```
% Gaussian Process Regression model
gprMdl = fitrgp(Strain, Stress, 'BasisFunction', 'linear', 'KernelFunction', 'squaredexponential', 'FitMethod',
'exact', 'PredictMethod', 'exact');

% Predict the stress values for the extrapolated strain
[extrapolatedStress, ~] = predict(gprMdl, extrapolatedStrain);

% Append the extrapolated data to the original data
Strain = [Strain; extrapolatedStrain];
Stress = [Stress; extrapolatedStress];

% Plot the original and extrapolated stress-strain curve
figure;
plot(Strain, Stress, 'b-', 'LineWidth', 2);
hold on;
plot(extrapolatedStrain, extrapolatedStress, 'r--', 'LineWidth', 2);
legend('Original Curve', 'Extrapolated Curve');
title('Stress vs. Strain with GPR Extrapolation');
xlabel('Strain');
ylabel('Stress (Pa)');
grid on;
%% Stiffness 75%-80%
close all

[~,newstartIdx] = min(abs(Strain-0.75));
[~,newendIdx] = min(abs(Strain-0.80));
highstrain = Strain(newstartIdx+1:newendIdx);
highstress = Stress(newstartIdx+1:newendIdx);
[ultimateStress, idxUltimate] = max(highstress);  % max function also returns the index of the max value
ultimateStrain = highstrain(idxUltimate);

% Plot the stress-strain curve for this range
figure;
plot(highstrain, highstress, 'b-', 'LineWidth', 2);
%title(sprintf('Stress vs. Strain (75%%-80%%), Ultimate Stress: %.2f Pa at %.2f%% Strain', ultimateStress,
ultimateStrain*100));
xlabel('Strain');
ylabel('Stress (Pa)');
```